TC.
DOKUZ EYLUL UNIVERSITY
IZMIR INTERNATIONAL
BIOMEDICINE AND GENOME
INSTITUTE

THE INTERROGATION OF THE ROLE OF MALT1 PARACASPASE (MUCOSA-ASSOCIATED LYMPHOID TISSUE LYMPHOMA TRANSLOCATION PROTEIN 1) IN HEPATOCELLULAR CARCINOMA CELL SURVIVAL

ASLI KURDEN PEKMEZCI

MOLECULAR BIOLOGY AND GENETICS

MASTER DISSERTATION

IZMIR-2019

2016850002

TC.
DOKUZ EYLUL UNIVERSITY
IZMIR INTERNATIONAL
BIOMEDICINE AND GENOME
INSTITUTE

THE INTERROGATION OF THE ROLE OF MALT1 PARACASPASE (MUCOSA-ASSOCIATED LYMPHOID TISSUE LYMPHOMA TRANSLOCATION PROTEIN 1) IN HEPATOCELLULAR CARCINOMA CELL SURVIVAL

MOLECULAR BIOLOGY AND GENETICS

MASTER DISSERTATION

ASLI KURDEN PEKMEZCI

Assoc. Prof. Serif Senturk

2016850013

YÜKSEK LİSANS TEZ SAVUNMA SINAVI TUTANAĞI

Dokuz Eylül Üniversitesi İzmir Uluslararası Biyotıp ve Genom Enstitüsü Genom Bilimleri ve Moleküler Biyoteknoloji Anabilim Dalı Yüksek Lisans Programı 2016850013 numaralı öğrencisi Aslı KURDEN PEKMEZCİ, "MALT1 PARAKASPAZIN (MUCOSA-ASSOCIATED LYMPHOID TISSUE LYMPHOMA TRANSLOCATION PROTEIN 1) HEPATOSELÜLER KARSİNOM HÜCRE SAĞKALIMI ÜZERİNDEKİ ROLÜNÜN ARAŞTIRILMASI" konulu Yüksek Lisans tezini 24.07.2019 tarihinde yapılan savunma sınavı sonucunda başarılı olmuştur.

BAŞKAN
Doç. Dr. Şerif ŞENTÜRK
Dokuz Eylül Üniversitesi İzmir Uluslararası Biyotıp ve Genom Enstitüsü
Genom Bilimleri ve Moleküler Biyoteknoloji Anabilim Dalı

ÜYE
Doç. Dr. Özden Yalçın ÖZUYSAL
İzmir Yüksek Teknoloji Enstitüsü Fen
Fakültesi, Moleküler Biyoloji ve Genetik
Bölümü

ÜYE
Yrd. Doç. Dr. Yavuz OKTAY
Dokuz Eylül Üniversitesi Tıp Fakültesi
Temel Tıp Bilimleri Bölümü Tıbbi
Biyoloji Anabilim Dalı

TABLE OF CONTENTS

LIST OF TABLES

LIST OF FIGURES

ABBREVIATIONS

HCC: Hepatocellular Carcinoma

MALT1: Mucosa-Associated Lymphoid Tissue Lymphoma Translocation Protein 1

TERT: Telomerase reverse transcriptase

HCV: Hepatitis C virus

HBV: Hepatitis B virus

Nf-κB: Nuclear factor kappa light chain enhancer of activated B cells

MKi: Multiple kinase inhibitor

FDA: Food and drug administration

VEGFR: Vascular endothelial growth factor receptor

PDGFR: platelet-derived growth factor receptor

PD-1/PD-L1: programmed cell death protein 1/programmed death-ligand 1

CTLA-4: cytotoxic T-lymphocyte-associated protein 4

HGF: Hepatocyte growth factor

TNF-α: Tumor necrosis factor alpha

IκB: Inhibitor of kB

IKK: IκB kinase

TRAF6: Tumor necrosis factor receptor-associated factor 6

shRNA: Short hairpin Ribonucleic acid

gRNA: Guide RNA

ACKNOWLEDGEMENTS

July 2019   Asli KURDEN PEKMEZCI

THE INTERROGATION OF THE ROLE OF MALT1 PARACASPASE (MUCOSA-ASSOCIATED LYMPHOID TISSUE LYMPHOMA TRANSLOCATION PROTEIN 1) IN HEPATOCELLULAR CARCINOMA CELL SURVIVAL

Asli Kurden Pekmezci, Dokuz Eylul University Izmir International Biomedicine and Genome Institute, asli.kurden@msfr.ibg.edu.tr

ABSTRACT

Hepatocellular carcinoma (HCC) is a leading cause of cancer related deaths around the world and is associated with several etiological factors including infections with hepatitis B and C viruses, heavy alcohol consumption and chronic aflatoxin B1 exposure. Treatment strategies for HCC are currently limited. Hepatocarcinogenesis process involves alterations in several molecular pathways including activation of NF-κB pathway. MALT1 (Mucosa-Associated Lymphoid Tissue Lymphoma Translocation Protein 1) is a cytosolic signaling molecule which acts both as a scaffold protein and as a protease for NF-κB pathway activation. To date, the contribution of MALT1 to HCC cell survival has not been studied. In the present study, we investigated the effects of MALT1 inhibition on HCC cell survival. For this purpose, we depleted the MALT1 levels in HCC cell lines via three strategies; RNAi, CRISPR-Cas9 and small molecule inhibitor and we analyzed the cell survival with different methods. Based on the preliminary results, shRNA-mediated gene silencing or pharmacological inhibition with MI-2 reduced cell growth in vitro, and this decrease in cell growth is associated with inhibition of cell proliferation as well as reduced expression of well-known NF-kB downstream targets, an indirect indication of NF-κB pathway inactivation. Besides, we performed a competition assay using CRISPR-Cas9 system in order to test MALT1 dependency in HCC cells. Conclusively, our results suggest that MALT1 plays an important role in HCC cell growth. Further studies focusing on delineating the molecular mechanisms underlying the growth regulating effects of MALT1 are currently underway. By all means, we think that pharmacological inhibition of MALT1 in HCC is a promising avenue to be explored further.

Key Words: Hepatocellular carcinoma, NF-κB, MALT1, RNAi, CRISPR

MALT1 PARAKASPAZIN (MUCOSA-ASSOCIATED LYMPHOID TISSUE LYMPHOMA TRANSLOCATION PROTEIN 1) HEPATOSELÜLER KARSINOM HÜCRE SAĞKALIMI ÜZERINDEKI ROLÜNÜN ARAŞTIRILMASI

Aslı Kurden Pekmezci, Dokuz Eylül Üniversitesi İzmir Uluslararası Biyotıp ve Genom Enstitüsü, asli.kurden@msfr.ibg.edu.tr

<u>ÖZET</u>

Hepatoselüler karsinom (HSK), dünyadaki kansere bağlı ölümlerin önde gelen nedenlerinden biridir ve hepatit B ve C virüsleri enfeksiyonları, ağır alkol tüketimi ve kronik aflatoksin B1 maruziyeti dahil olmak üzere birçok etyolojik faktörle ilişkilidir. Günümüzde HSK için tedavi stratejileri sınırlıdır. Hepatokarsinogenez sürecinde, NF-κB yolağının aktivasyonu da dahil olmak üzere birçok moleküler yolakta değişiklikler gözlenir. MALT1 (Mucosa-Associated Lymphoid Tissue Lymphoma Translocation Protein 1), NF-κB yolağında rol alan ve bu yolağın aktivasyonunda hem iskele proteini hem de proteaz olarak görev yapan bir sitozolik sinyal molekülüdür. MALT1'in HSK hücre sağkalımına katkısı bugüne kadar çalışılmamıştır. Bu çalışmada MALT1 inhibisyonunun HSK hücre sağkalımı üzerindeki etkilerini araştırdık. Bu amaçla, HSK hücrelerinde MALT1 seviyelerini azaltmak için üç strateji uyguladık; RNAi, CRISPR / Cas9 ve küçük moleküllü inhibitor, ve ardından hücre sağkalımını farklı yöntemlerle analiz ettik. shRNA aracılı gen susturma veya MI-2 ile farmakolojik inhibisyonun, in vitro olarak hücre büyümesini azalttığını gözlemledik. Ön verilerimiz, hücre büyümesindeki bu düşüşün, NF-κB yolağının inaktivasyonunun dolaylı bir göstergesi sayılan, NF-κB hedef genlerinin ifadesinin azalmasıyla ve hücre proliferasyonunun inhibisyonu ile açıklanabileceğini göstermektedir. Ayrıca, HSK hücrelerinde MALT1 bağımlılığını test etmek için CRISPR-Cas9 sistemini kullanarak bir rekabet analizi uyguladık. Sonuç olarak, verilerimiz MALT1'in HSK hücre büyümesinde önemli bir rol oynadığını göstermektedir. İleriki çalışmalar, MALT1'in büyüme düzenleyici etkisinin altında yatan moleküler mekanizmaları tanımlamaya odaklanacaktır. HSK'de MALT1'in farmakolojik inhibisyonunun, daha fazla araştırılması gereken umut verici bir alan olduğunu düşünüyoruz.

Anahtar Kelimeler: Hepatoselüler karsinom, NF-κB, MALT1, RNAi, CRISPR

1. INTRODUCTION

1.1. Hepatocellular Carcinoma

Liver cancer is the sixth most common cancer and is a leading cause of cancer related deaths around the world. Hepatocellular carcinoma is the most common primary liver cancer and it accounts for 75%-85% of the cases.[1] Hepatocarcinogenesis is a complex multistep process which involves alterations in a several molecular pathways, and finally leads to HCC progression.[2] The most affected pathways in hepatocarcinogenesis are WNT-β-catenin, phosphoinositol-3-kinase/Akt, hedgehog, p53 and c-Met pathways.[3]
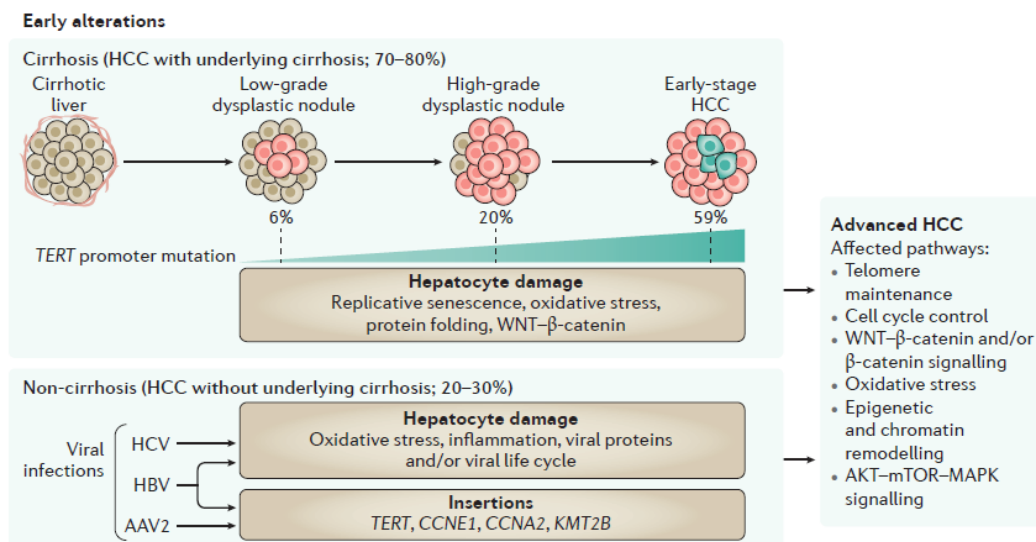
Figure 1. Hepatocarcinogenesis process.[2]

In cirrhotic liver, the process starts with the development of low-grade dysplastic nodules (LGDNs) followed by the development of high-grade dysplastic nodules. The nodules then transform into early stage HCC. During this transformation, several changes observed in hepatocytes as activation of WNT-β-catenin pathway. These changes separate early stage HCC from the dysplastic nodules.[2] TERT promoter mutations are also required to promote hepatocarcinogenesis.[4] Moreover, viral infections cause molecular alterations associated with malignant transformation. These infections either damage hepatocytes by viral protein expression, inflammation etc., or cause mutagenesis via genomic insertions to certain hepatocarcinogenesis related genes.[2]

1.1.1. Risk Factors

Today, several risk factors for HCC and their mechanisms have been defined. In 80-90% of the cases, HCC develops from cirrhosis, the main causes of which are HCV and HBV infections.[5] Cirrhosis occurs when hepatocytes lose their proliferative capacity and undergo necrosis. This causes liver to lose its regenerative capacity and leads to fibrosis.[3] 50% of HCC cases are associated with HBV infection and around 25% of them are caused by HCV infection.[3]

Hepatitis B virus infection can increase the risk for HCC up to 100-fold.[6] HBV can induce hepatocarcinogenesis in two ways. The first is an indirect mechanism in which the infection damages hepatocytes and causes inflammation and oxidative stress. This damage causes accumulation of mutations, such as oncogene activation, and therefore contributes to liver damage such as fibrosis, cirrhosis and eventually tumor initiation.[3,7] Second, HBV can directly promote hepatocarcinogenesis without cirrhosis by integrating its DNA into host genome which induces mutations and chromosomal rearrangements. Besides, its regulatory protein HBx, which is a viral oncoprotein, interacts with number of signaling pathways such as WNT-β-catenin, p53 and Nf-κB pathways. By this means, it contributes to cancer cell proliferation and HCC development.[8]

Hepatitis C virus infected patients have around 20-30-fold higher risk for developing HCC.[5] Unlike HBV, HCV is an RNA virus and is unable to integrate its DNA into host genome.[3] HCV core proteins can interact with host's tumor suppressor proteins such as p53 and pRb and promotes proliferation. Also, HCV core can regulate several molecular pathways including WNT-β-catenin, Raf/MAPK, and NF-κB, leading to proliferation, inflammation and tumor formation.[9]

Other risk factors include nonalcoholic fatty liver disease, nonalcoholic steatohepatitis, aflatoxin B1 exposure, alcohol consumption, and obesity.[10]

1.1.2. Current Treatment Modalities for HCC

Liver transplantation, resection, and local ablative therapies can be performed only in early stages of HCC. Unfortunately, HCC is often diagnosed in advanced stage. Patients with advanced HCC need systemic treatments.[11] Especially, Tyrosine Kinases (TKs) and Cyclin-Dependent Kinases, which are crucial for proliferation and metabolism, are dysregulated in hepatocellular carcinoma. Therefore, these kinases are being targeted by several approved drugs for the HCC treatment.[10]

Sorafenib is the first systemic drug for the treatment of HCC, approved by FDA in 2007. It is an orally active multikinase inhibitor (MKi) which targets VEGFR (vascular endothelial growth factor receptor), PDGFR (platelet-derived growth factor receptor), and Raf kinase.[11] Sorafenib has been successful in increasing overall survival however, most patients develop drug resistance and could not benefit from the therapy.[10,12]

Regorafenib, which has similar targets as sorafenib, approved as an oral MKI for unresectable HCC in June 2017. It has shown a better performance in terms of tyrosine kinase inhibition, patient survival benefits and drug tolerance. Currently, it is a standard treatment for the sorafenib refractory patients.[10,12]

Lenvatinib is another FDA approved (in US) MKi that targets VEGFR, FGFR, PDGFR, KIT, and RET. In clinical trials it was non-inferiority to sorafenib, however it is a more potent inhibitor and has a broader range of targets.[13] Cabozatinib, on the other hand, was approved in Europe in 2018 for the patients treated with sorafenib. It targets RET, VEGFR, MET, and AXL as a MKi.

Further, there are studies and clinical trials assessing monotherapies (linifanib, sunitinib, brivanib) or combination therapies with sorafenib (erlotinib). However they did not show, so far, a superior effect compared to sorafenib alone.[13] Besides, several systemic drugs were assessed (everolimus, tivantinib, ramucirumab, brivanib) for the sorafenib intolerant patients, but trials did not show any benefit as to placebo (Figure 2).[14]
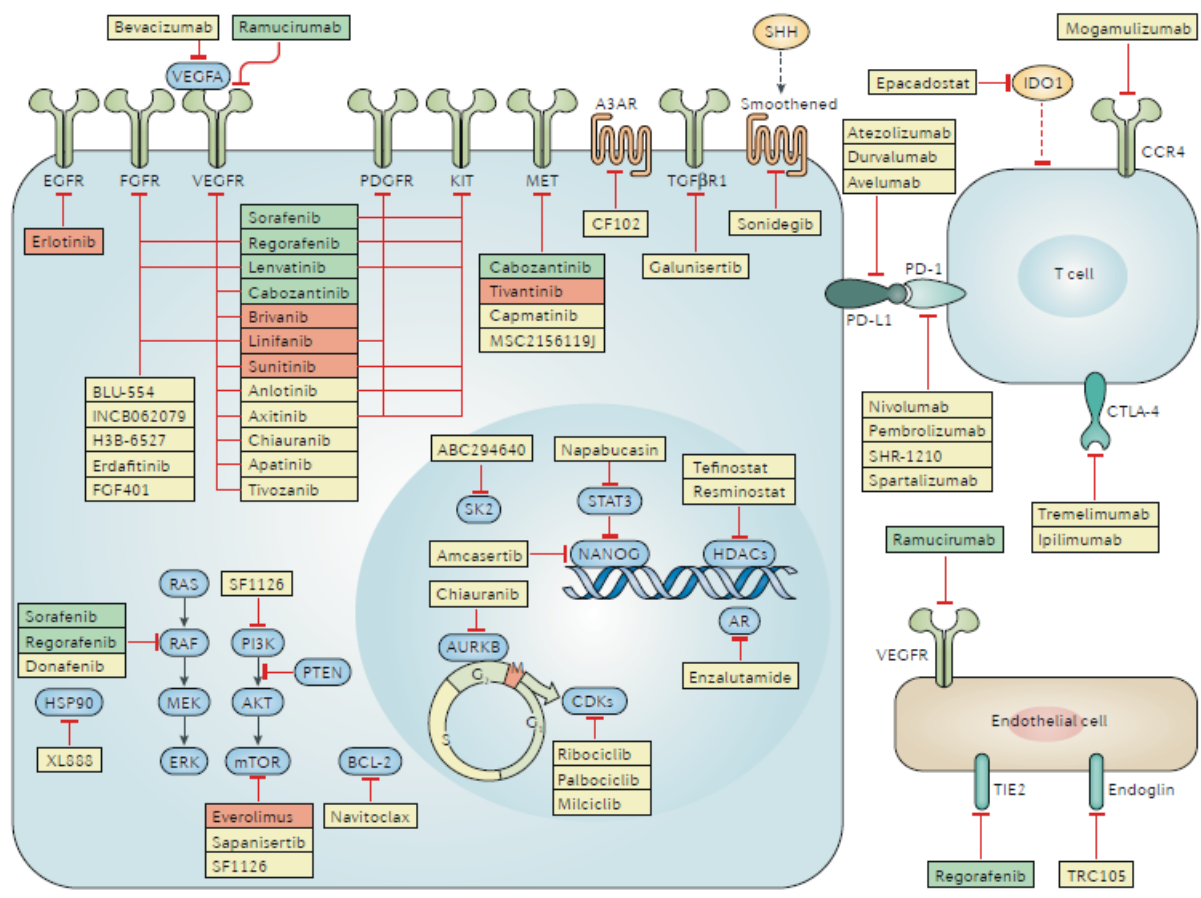
Figure 2. Current drugs for HCC. Green boxes inidicate positive results from trials Red boxes show negative results. Drugs in yellow boxes are being tested currently in HCC. [15]

Beside MKis, immune checkpoint inhibitors are another treatment strategy for HCC. They block, in particular, the ligand-receptor interaction between the tumor cells and T cells, thereby leading to the activation of immune cells to target and kill the tumor cells. Two types of immune checkpoints have been targeted to date; PD-1/PD-L1 receptors (programmed cell death protein 1/programmed death-ligand 1) and CTLA-4 (cytotoxic T-lymphocyte-associated protein 4).[14,16] Nivolumab, tislelizumab, camrelizumab, pembrolizumab, atezolizumab and durvalumab belong to the first group of immune checkpoint inhibitors; tremelimumab and ipilimumab are the antibodies against CTLA-4.[15,16] Currently, two PD-1 blocking immune checkpoint inhibitors, Nivolumab and Pembrolizumab are the approved for the HCC treatment.[17]

1.2. NF-κB Pathway

One of the dysregulated pathways in human cancers, including HCC, is NF-κB pathway which controls the expression of number of genes related to survival, proliferation, apoptosis, immune response etc.[18] It has been shown that the both HBV and HCV infections could lead to activation of NF-κB pathway in primary hepatocytes and it is thought that this activation could play role in hepatocarcinogenesis process.[19–21] The activation of NF-κB pathway in the hepatocytes could be due to a direct effect of HBV/HCV core proteins or a paracrine effect. In the second case the infection causes an inflammatory response in kupffer and/or stellate cells, and they secrete several hepatomitogens such as IL-6, Hepatocyte growth factor (HGF) and TNF-α, which promote NF-κB activation and proliferation of transformed hepatocytes.[21,22]
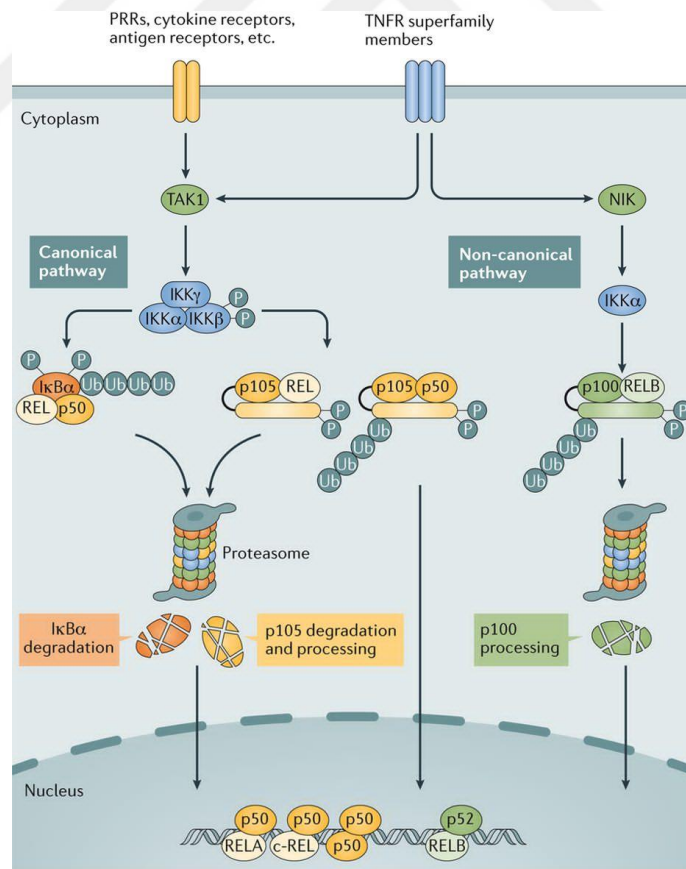
Figure 3. NF-κB pathway.[23]

NF-κB transcription factor family consists of 5 different dimers; namely NF-κB1 (p105 and p50), NF-κB2 (p100 and p52), c-Rel, RelA (p65), and RelB. Their activations are regulated by a group of inhibitory proteins, IκB family, which are degraded by an IκB kinase (IKK) complex. Degradation of IκB frees the NF-κB family members which then translocate to the nucleus and induce gene transcription.[19,24]

NF-κB pathway activation occurs mainly in two ways; canonical and non-canonical pathways (Figure 3). Canonical pathway can be activated by number of proinflammatory cytokines and cellular stresses. Upon stimulation, IKK complex is activated by phosphorylation via TGF-b-activated kinase 1 (TAK1) or MAPK kinase kinase 3 (MEKK3), and β subunit of the IKK complex phosphorylates IκBα which is then degraded via ubiquitination/proteasome dependent processing. This causes NF-κB p65 and p50 to translocate to the nucleus and promote DNA binding and target gene transcription.[25,26] The non-canonical pathway responds only to a set of cytokines which belong to TNF superfamily.[18] After stimulation, NF-κB inducing kinase (NIK) activates IKKα which phosphorylates p100 to generate p52. RelB forms a dimer with p52, this NF-κB complex enter the nucleus to induce target gene expression.[25]

NF-κB pathway can be regulated in several ways. To date, several kinases were shown to phosphorylate and thereby activate p65; namely protein kinase A, mitogen and stress activated kinase protein kinase 1/2 (MSK1/2), IKKα/β, PKCζ, TRAF-family-member associated (TANK)-binding kinase 1 (TBK1).[24,27] On the other hand, histone deacetylases, HDAC1/2/3, repress transactivation by acetylating p65, leading to inactivation of NF-κB.[27] One of the regulators of the NF-κB pathway is MALT1 (mucosa-associated lymphoid tissue lymphoma translocation protein 1). MALT1 activates the pathway by cleaving the negative regulators such as A20, CYLD, RelB, Regnase-1 and NIK.[28]

1.2.1. MALT1

MALT1 is firstly discovered in MALT lymphomas and since then it has been studied mainly in immune cells especially T and B cells. It is a paracaspase with an N-terminal death domain, and a C-terminal caspase-like domain similar to proteases of the caspase

family, both followed by immunoglobulin-like domains (Figure 3). Outside the protease domain it has also a binding motif for TRAF6, which promotes IKK complex activation.[29]
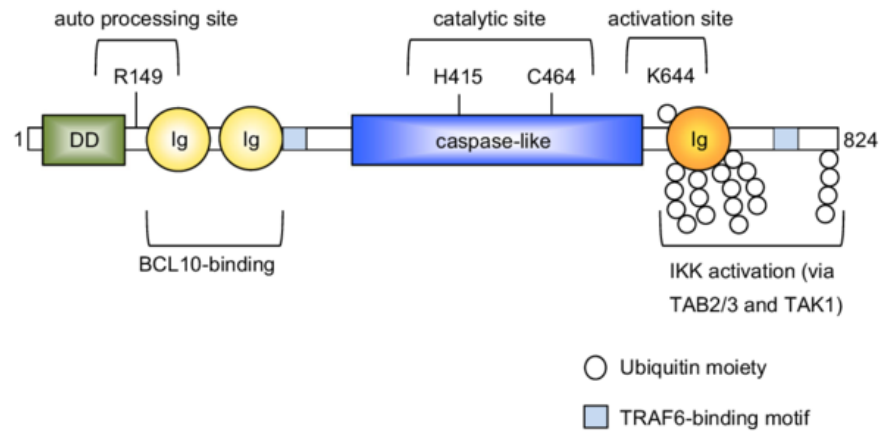
Figure 4. Structural domains of MALT1.[29]

As a scaffolding protein; MALT1 forms a complex with CARMA1/3 or CARD9 and Bcl10 namely CBM complex, leading to TRAF6 recruitment and IKK complex activation, which eventually leads to NF-κB pathway activation.[30] The CBM complex formation can be induced by different type of receptors, not restricted to only T and B cell receptors. G protein coupled receptors (GPCRs), receptor tyrosine kinases (RTKs) and epidermal growth factor receptors (EGFRs) can trigger the complex formation and MALT1 activation in non-immune cells.[29–31] Alternatively MALT1 can be activated without the CBM complex formation. Two recent studies suggested that MALT1 can be activated by a signaling cascade through a TNF superfamily receptor member OX40 in a TRAF6 dependent manner[32] and by interacting with Kaposi's sarcoma associated herpes virus (KSHV) proteins[33]. The latter also showed that the binding of viral proteins to MALT1 lead to NF-κB activation and inhibition of protease function of MALT1 induced the viral lytic cycle and decreased cell viability in primary effusion lymphoma cells.[33]

MALT1 has also a protease activity and to date several proteolytic substrates of MALT1 have been discovered. One of them is RelB which inhibits NF-κB pathway by forming dimers with RelA and c-Rel, masking their DNA binding ability or by competitive DNA binding. MALT1 dependent cleavage of RelB leads to activation of NF-κB pathway.[34]

Two deubiquitinating enzymes A20 and CYLD which remove polyubiquitin chains from key signaling molecules, such as MALT1, TRAF6, NEMO, are also targets for MALT1. Their cleavage results in NF-κB activation and increased cell survival.[31,34] In certain lymphomas MALT1 fuses with cIAP2 protein and gains ability to cleave NIK in the non-canonical NF-κB pathway resulting in activation of this pathway.[34] MALT1 indirectly plays a role in posttranscriptional regulation by cleaving RNase regnase-1 (MCPIP1) and roquin which destabilize mRNAs of multiple genes such as IL-6, IL-2 and c-Rel. Besides other targets, MALT1 also cleaves itself, owing to its auto-processing site. This auto-cleavage activates NF-κB pathway in a TRAF6 dependent manner, however the exact mechanism has not been clarified yet.[29,34]

So far, the functions of MALT1 have been studied extensively in immune cells. However several other studies showed the importance of MALT1 in cell survival in other tumor types as lung cancer[35], oral squamous cell carcinoma (OSCC)[36] and ovarian cancer[37]. MALT1 dependent NF-κB pathway activation in different cell types is a promising area for future research, since number of activation mechanisms of MALT1 have been found other than T and B cell receptor mediated ones.[38] Also having a minor functional and structural homology to other proteins, MALT1 has an advantage as a therapeutic target.[34]

1.3. Aim of The Study

The aim of the study was to investigate the role of MALT1 paracaspase in Hepatocellular carcinoma cell survival. To achieve this goal, we depleted MALT1 in HCC cells via 3 methods; RNAi system, CRISPR-Cas9 system and small molecule inhibitor. We investigated the cell viability decrease by Crystal violet staining after MALT1 knock-down. We monitored the edited cell percentage in a cell population after CRISPR-Cas9 editing, via competition assay. We finally determined the viability of cells after small molecule inhibitor treatment, via XTT cell viability assay.

2. MATERIALS & METHODS

2.1. MATERIALS

2.1.1. Patient cDNA Samples

Patient cDNA samples were kindly provided by Prof. Dr. Neşe ATABEY.

2.1.2. Cell Lines

Huh7, Hep40, HepG2, Hep3B, Hep3B-TR, PLC/PRF/5, SNU182, SNU387, SNU398, SNU423, SNU449, SNU475, Mahlavu, Sk-Hep1 and Focus HCC cell lines and Hek293T cell line were kindly provided by Prof. Dr. Mehmet Öztürk (Izmır Biomedicine and Genome Center) and Assoc. Prof. Dr. Nuri Öztürk (Gebze Technical University), respectively.

2.1.3. Oligonucleotides

The oligonucleotides, synthesized by Macrogen (Ankara, Turkey), were listed in Table 1. shMALT1-2 and shRPA3 sequences were obtained from Sigma-Aldrich (https://www.sigmaaldrich.com/). shRPA3 was used as a positive control since it targets the RPA3 gene whose protein is essential during the DNA replication. gRNAs were designed by using the online CRISPR gRNA design tool http://crispr.mit.edu/ developed by Feng Zhang lab, Massachusetts Institute of Technology (Figure 5). "CACC" and "AAAC" BsmBI recognition sites were added to upstream of forward and reverse oligonucleotides, respectively. One "G" was added after the recognition site and one "C" was added to the end of the oligonucleotide since BsmBI enzyme cuts one base after recognition site. gRNAs were numbered from the starting base of MALT1-202 transcript (ID: ENST00000348428.7). gRen was used as a negative control since it targets the Renilla gene which human genome does not contain. gRPA3 was used as a positive control.

Table 1. List of oligonucleotides used in this study.

Name	Sequence (5'→3')
shMALT1-2_F	CCGGCTACGATGATACCATTCCAATCTCGAGATTGGAATGGTATCATCGTAGTTTTTG

shMALT1-2_R	AATTCAAAAACTACGATGATACCATTCCAATCTCGAGATTGGAATGGTATCATCGTAG
shRPA3_F	CCGGGATCTTGGACTTTACAATGAACTCGAGTTCATTGTAAAGTCCAAGATCTTTTTG
shRPA3_R	AATTCAAAAAGATCTTGGACTTTACAATGAACTCGAGTTCATTGTAAAGTCCAAGATC
gRen_F	CACCGGTAGCGCGGTGTATTATACC
gRen_R	AAACGGTATAATACACCGCGCTACC
gMALT1-258_F	CACCGGCGAGGGCCATGTCGCTGTT
gMALT1-258_R	AAACAACAGCGACATGGCCCTCGCC
gMALT1-259_F	CACCGCGAGGGCCATGTCGCTGTTG
gMALT1-259_R	AAACCAACAGCGACATGGCCCTCGC
gMALT1-268_F	CACCGCGGGTCCCCCAACAGCGACA
gMALT1-268_R	AAACTGTCGCTGTTGGGGGACCCGC
gMALT1-272_F	CACCGGCTGTTGGGGGACCCGCTAC
gMALT1-272_R	AAACGTAGCGGGTCCCCCAACAGCC
gRPA3_F	CACCGGATGAATTGAGCTAGCATGC
gRPA3_R	AAACGCATGCTAGCTCAATTCATCC

U6_F	GAGGGCCTATTTCCCATGATT
MALT1_F	GACCCATTCCATGGTGTTTACC
MALT1_R	AATAAATGCATCTGGAGTCCGG
IL6_F	AACCTGAACCTTCCAAAGATGG
IL6_R	TCTGGCTTGTTCCTCACTACT
RPL41_F	GAAACCTCTGCGCCATGA
RPL41_R	TCTTTCTTCTTTTGCGCTTCA
CCL2_F	CAGCCAGATGCAATCAATGCC
CCL2_R	TGGAATCCTGAACCCACTTCT
AFP_F	AGGGAGCGGCTGACATTATT
AFP_R	GGCCAACACCAGGGTTTACT

Figure 5. shRNA positions on the MALT1 mRNA. shMALT1-1 and shMALT1-2 target exon 5 and exon 12, respectively.
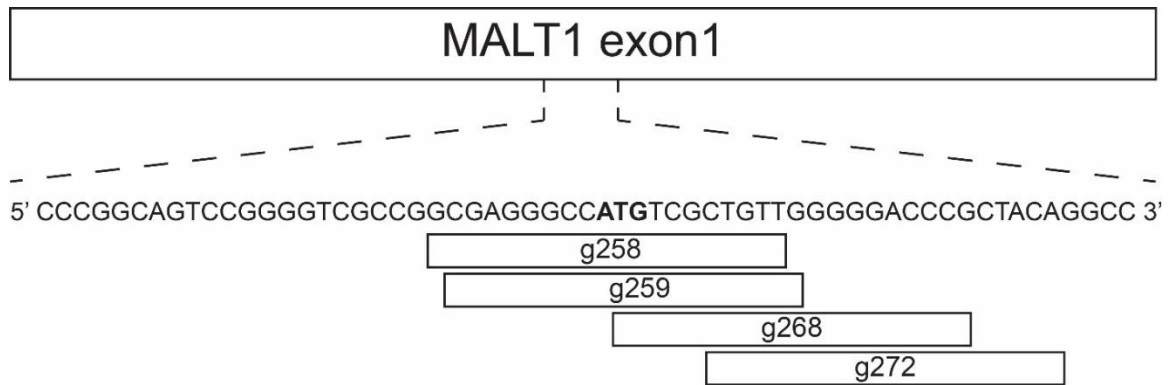
Figure 6. gRNA locations in MALT1 exon1.

2.1.4. Plasmids

The plasmids used in this study are listed in Table 2.

Table 2. Plasmids used in the study.

Name	Source
pLKO.1-puro_empty	Addgene #8453
pLKO.1_shSCR	Addgene #17920
pLKO.1_shMALT1-1	Sigma
pECPV[39]	Senturk, Serif, et al., 2017
pMD2G	Addgene #12259
psPAX2	Addgene #12260
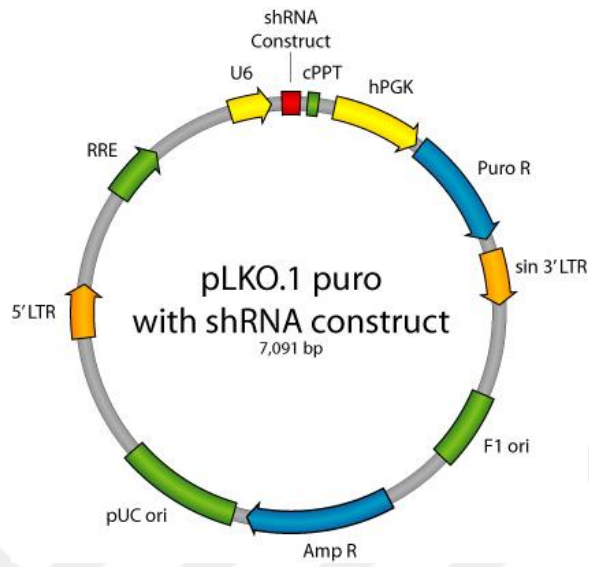
Figure 7. pLKO.1 vector map.[40]
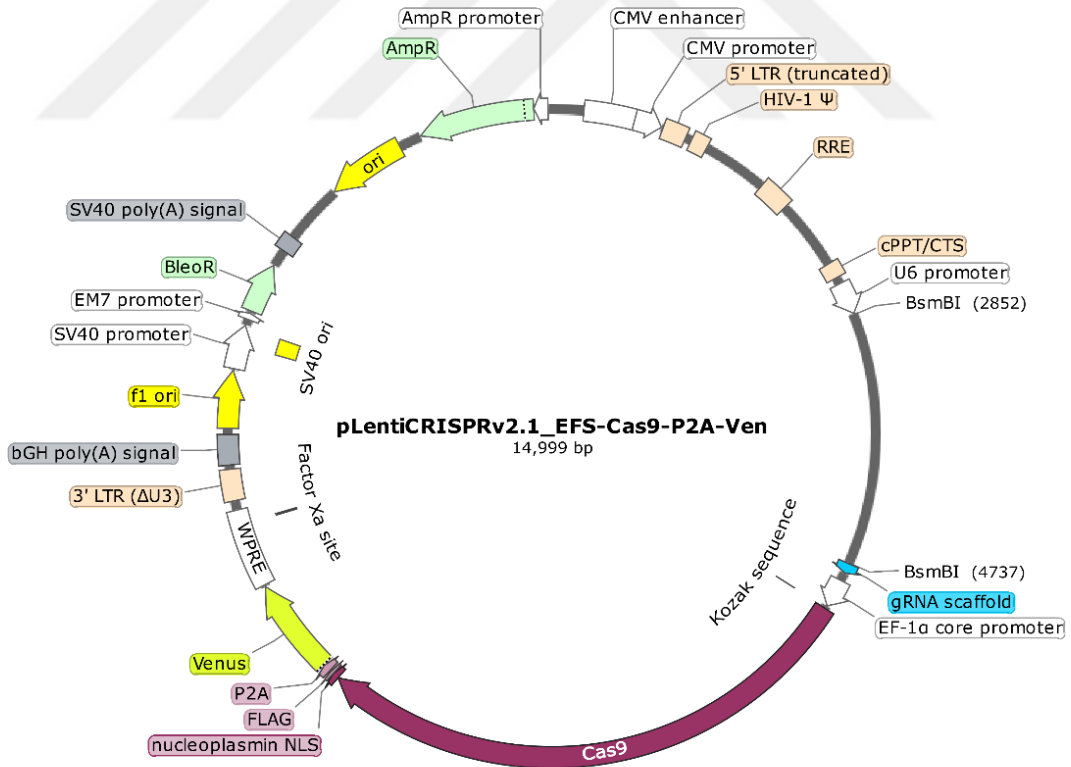
Figure 8. pECPV vector map.
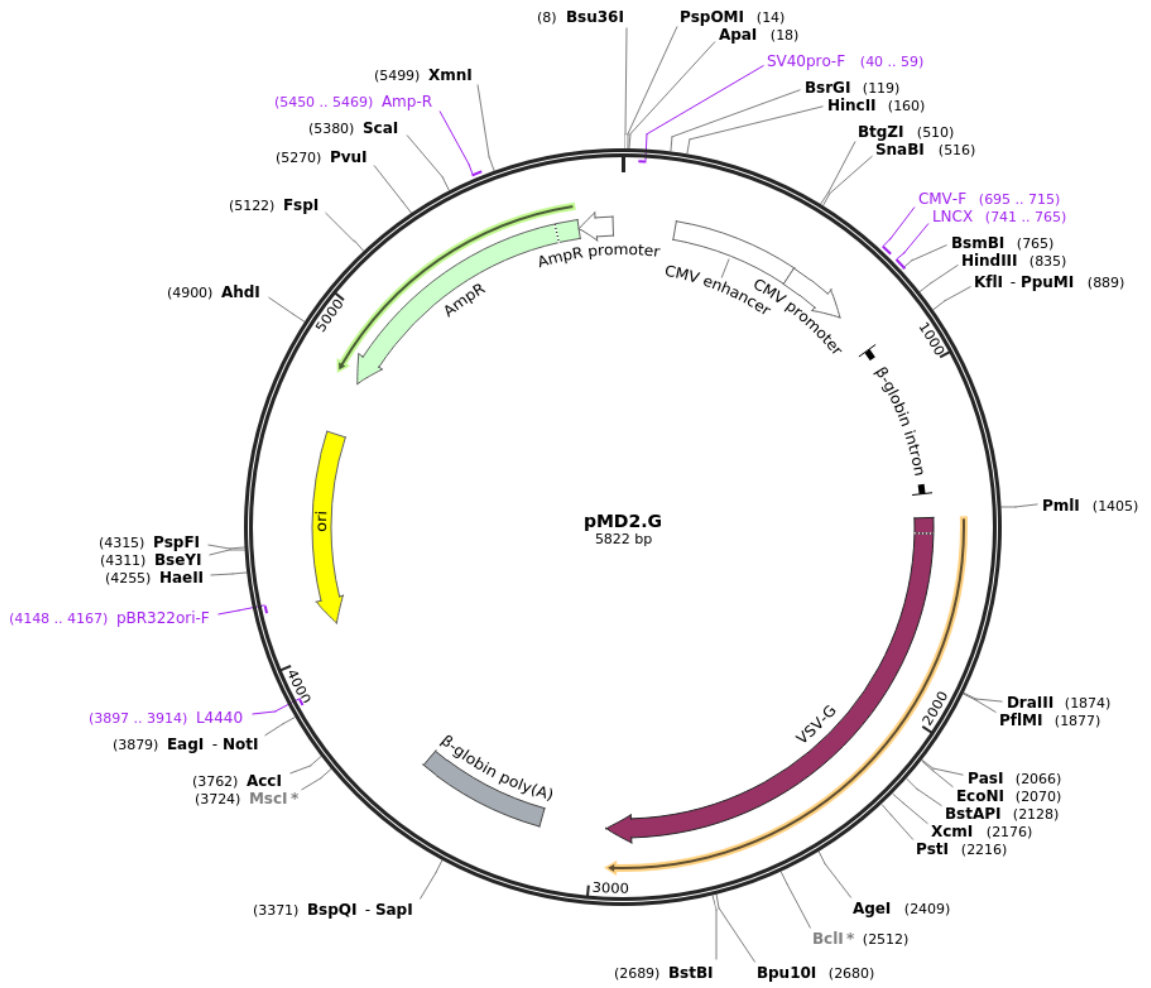
Figure 9. pMD2.G packaging helper vector map.[41]
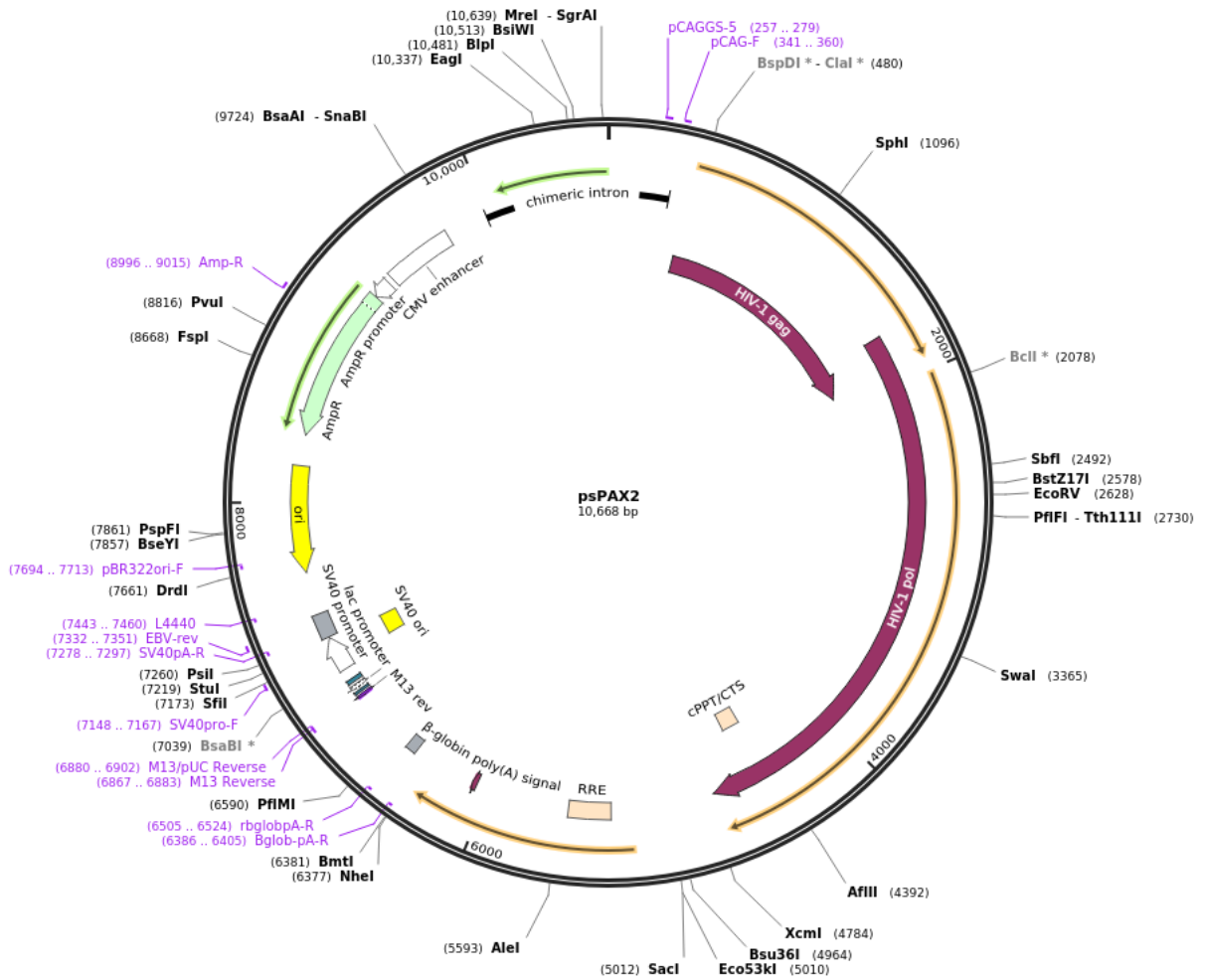
Figure 10. psPAX2 helper vector map.[42]

2.1.5. Bacterial Strains

DH10b Competent *Escherichia coli* (C3019I, New England Biolabs, USA) strain was used with pSPAX helper vector and Invitrogen™ One Shot™ Stbl3™ chemically competent strain (C737303, Thermo Fisher Scientific, USA) was used with pLKO.1, pECPV and pMD2.G vectors.

2.1.6. Reagents for Bacterial Experiments

Luria-Bertani (LB) media, LB agar plates, and antibiotic stocks were used for bacterial experiments. Recipes were listed on the Table 3.

Table 3. Recipes of reagents used in bacterial experiments.

Reagents	Recipe
LB Media	10g NaCl, 5g yeast extract and 10g tryptone were dissolved in 1 L ddH$_2$O. Autoclaved.
Ampicillin Stock (100mg/ml)	1000mg ampicillin was dissolved in 10ml ddH$_2$O. Filtered and aliquots were stored at -20°C.
LB Agar plates	35 g (3.5%) LB broth with agar was dissolved in 1L ddH$_2$O. It was heated and stirred. Sterilized by autoclaving. Cooled to 55°C. 1 ml of the 100mg/ml ampicillin stock was added. Poured into petri dishes ($\approx$ 15 ml per 100 mm dish).

2.1.7. Enzymes & Buffers

Enzymes and buffers used in this study are listed in Table 4.

Table 4. Enzymes & Buffers

Name	Catalog Number	Vendor
AgeI	R3552S	New England Biolabs
CutSmart® Buffer	B7204S	New England Biolabs
EcoRI	R3101S	New England Biolabs
Fast Digest BsmbI	FD0454	Thermo Fisher Scientific

FastAP Thermosensitive Alkaline Phosphatase	EF0651	Thermo Fisher Scientific
FastDigest Buffer	B64	Thermo Fisher Scientific
RNaseA		
T4 DNA Ligase	M0202S	New England Biolabs
T4 DNA Ligase Reaction Buffer	B0202S	New England Biolabs
T4 Polynucleotide Kinase	M0201S	New England Biolabs
Taq polymerase	EP1701	Thermo Fisher Scientific

2.1.8. Cell Culture Materials & Reagents

Tissue culture plates, dishes, serological pipettes, and cryovials were obtained from Sarstedt (Nümbrecht, Germany) or SPL Life Sciences, Korea. Other cell culture materials are listed in Table 5.

Table 5. Cell culture materials

Name	Catalog Number	Vendor
0,45µm PES membrane filter	AND2545	Gilson
DMEM	41965039	Gibco
DMSO	472301-100ML	Sigma
FBS	10500064	Gibco
Lipofectamine™ 3000 Transfection Reagent	L3000015	Invitrogen
PBS	70011036	Gibco
Penicillin-Streptomycin	15140122	Gibco
Polybrene	H9268-5G	Sigma
RPMI	21875034	Gibco
TrypLE Express Enzyme	12604013	Gibco

2.1.9. Chemicals and Commercial kits

Chemicals and commercial kits used in this study are listed in Table 6.

Table 6. Chemicals & Commercial kits

Name	Catalog Number	Vendor
100bp DNA Ladder	N3231S	New England Biolabs
1kb DNA Ladder	N3232S	New England Biolabs
Acetic acid	27225-2.5L-R	Sigma
Agarose	A9539-100G	Sigma
Ampicillin	A0166	Sigma
Aprotinin (5mg/ml)	1278-25mg	Neofroxx
Crystal Violet	C6158	Sigma
Deoxynucleotide (dNTP) Solution Mix	N0447S	New England Biolabs
EDTA	E5134-500G	Sigma
EGTA (0,1M)	E3889-10G	Sigma
Ethanol	920.026.2500	Isolab
Formaldehyde	F1635-500	Honeywell
Gel Loading Dye, Purple (6X)	B7024S	New England Biolabs
Glycine	sc29096A-500g	Santa Cruz
iScript™ cDNA Synthesis Kit	1708891	Bio-Rad
Isopropanol	24137-2.5L-R	Sigma
LB Broth with Agar	L2897-1KG	Sigma
Leupeptin	1273-25mg	Neofroxx
MI 2 (MALT1 inhibitor)	S7429	Selleckchem
Na deoxycholate	30970-25G	Sigma
Na Vanadate	sc-3540A	Santa Cruz
NaCl	M106404.1000	Merck
NaF	S6776-100G	Sigma
NucleoSpin® Gel and PCR Clean-up	740609.5	Macherey Nagel
NucleoSpin® Plasmid	740588.5	Macherey Nagel
NucleoSpin® RNA	740955.50	MN
Pepstatin	P5318-5MG	Sigma
PMSF	LSG36978-5G	Sigma
Propidium Iodide	81845	Sigma
RNase A	1263MG050	NeoFroxx

SDS	8170341000	Merck
Tris	T1503-1KG	Sigma
Triton X-100	t8787-100ml	Sigma
Tryptone	1553.05	AppliChem
XTT cell viability kit	30007	Biotium
Yeast Extract	MB16401	Nzytech
β-glycerolphosphate	50020-100G	Sigma

2.1.10. PCR reagents

Reagents used in PCR studies are shown in Table 7.

Table 7. PCR reagents

Name	Catalog	Vendor
iScript™ cDNA Synthesis Kit	1708891	Bio-Rad
BrightGreen 2X qPCR MasterMix-No Dye	MasterMix-S	abm
MicroAmp® Fast Optical 96-Well Reaction Plate	4346906	Thermo Fisher Scientific

2.1.11. Western Blot Reagents & Antibodies

Mini-PROTEAN® Tetra Cell and Mini Trans-Blot® Module system (Bio-Rad, #1658029) was used to perform Western Blot. Reagents and antibodies are listed in the Table 8 and Table 9 respectively.

Table 8. Reagents used in WB studies.

Name	Catalog number	Vendor
APS	1610GR100	BioFroxx
BLUeye Prestained Protein Ladder	PM007-0500	GeneDirex
Bovine serum albumin (BSA)	1126GR100	BioFroxx
Pierce™ BCA Protein Assay Kit	23227	Thermo Fisher Scientific

Ponceau S	P3504-10G	Sigma
Protogel	EC-890	National Diagnostics
Protogel stacking buffer	EC-893	National Diagnostics
Skimmed milk powder	70166-500G	Sigma
TEMED	T22500-100	Sigma
Tween-20	BP337-100	ThermoFisher
Nitrocellulose Membrane		

Table 9. Antibodies used in the WB studies.

Name	Cat number	Vendor
B-actin	ab8224	abcam
IRDye 680LT Donkey anti-Mouse IgG Secondary Antibody	926-68022	Li-Cor
IRDye 800CW Donkey anti-Rabbit IgG Secondary Antibody	92632213	Li-Cor
MALT1	sc46677	Santa Cruz Biotechnology
Phospho-Rb (Ser807/811)	9308S	Cell Signaling
α-Tubulin	sc-32293	Santa Cruz Biotechnology

RIPA lysis buffer, main gel buffer, sample loading buffer, running & transfer buffers, TBS and blocking & antibody diluting solutions were the solutions used in the WB studies. Recipes are listed in Table 10.

Table 10. Buffers used in WB studies.

Buffer	Recipe	
RIPA Lysis Buffer	Triton X-100 (10%)	5 ml
	Na deoxycholate (10%)	2,25 ml

	SDS (20%)	250 µl
	Tris-Cl pH 7,4 (1M)	2,5 ml
	NaCl (5M)	1,5 ml
	EDTA pH 8 (0,5M)	100 µl
	EGTA (0,1M)	500 µl
	β-glycerolphosphate (0,5M)	1 ml
	NaF (0,5M)	1 ml
	PMSF (0,1M)	500 µl
	Na Vanadate (0,1M)	500 µl
	Leupeptin (5mg/ml)	100 µl
	Aprotinin (5mg/ml)	100 µl
	Pepstatin (1mg/ml)	500 µl
	H_2O to final volume	
Main Gel Buffer	16 ml of 10% SDS 72,684g Tris - Add ddH2O to 180 ml - Adjust pH to 8,8 with HCl - Fill to 200 ml with ddH2O	
6X Laemmli sample loading buffer	Tris pH 6,8 (1 M) 15 ml SDS 2 g Glycerol 30 ml Bromophenol blue 0,3 g β-Mercaptoethanol 15 ml (add before use → 30% v/v)	
10X Running Buffer	250 mM Tris base 1,9 M Glycine 1% SDS pH~ 8,3	
10X Transfer Buffer	250 mM Tris base	

	1,9 M Glycine
	pH~ 8,3
10X TBS	24.23 g Trizma HCl
	80.06 g NaCl
	Mix in 800 ml of ultrapure water.
	pH to 7.6 with pure HCl.
	Top up to 1 L.
TBS-T	Dilute 10X TBS to 1X with dH2O. Add 1:1000 Tween-20.
Blocking solution	5% Skimmed milk powder in 1X TBS.
Antibody dilution solution	1% BSA (w/v) in 1X TBS-T

2.1.12. Hardware & Machines

Hardware and machines are listed in Table 11.

Table 11. Hardware & Machines

Machines	Vendors
Basic Power Supply	Biorad
MySpin™ 6 Mini Centrifuge	Thermo Scientific
Water Bath and Lid	Nüve
pH Meter	Hanna
Microwave Oven	Beko
SimpliAmp Thermal Cycler	Applied Biosystems
Vortex Mixer	Thermo Scientific
Electrophoresis Gel System	Biorad
Centrifuge 5810R	Eppendorf
Centrifuge MicroCL 17R	Thermo Scientific
Incubator MaxQ 4000	Thermo Scientific
Multiskan™ GO Microplate Spectrophotometer	Thermo Scientific

Nanodrop 2000	Thermo Scientific
GelDoc XR$^+$ with Image Lab Software	Biorad
Axio Vert.A1 Inverted Microscope	ZEISS
Li-Cor Odyssey Imaging System	Li-Cor
ABI 7500 Fast thermal cycler	Thermo Scientific
BD FACSAria™ III sorter	BD Biosciences
BD LSRFortessa™ cell analyzer	BD Biosciences

2.2. METHODS

2.2.1. Construction of shRNA and gRNA vectors

2.2.1.1. pLKO.1_shRNA vector construction

Annealing of oligonucleotide pairs

Forward and reverse shRNA oligonucleotide pairs were annealed in the following reaction mixture;

1,5 µl F oligo (100µM)   Annealing conditions;

1,5 µl R oligo (100µM)   4 min 95°C

5 µl 10X NEB2 Buffer   Ramp down to 25°C (0,1^{O}C/s)

42 µl ddH2O

Digestion of pLKO.1 vector

pLKO.1-Empty vector digested with AgeI and EcoRI in the following reaction mixture;

3µg pLKO.1-Empty vector

5 µl 10X CutSmart Buffer

35 µl ddH2O

1 µl AgeI-HF

1 µl EcoRI-HF

Digestion reaction; 8 hours, 37°C

Agarose gel electrophoresis & Gel purification

0,8% (w/v) agarose was weighed and mixed with 50ml 1X TAE buffer. Agarose was dissolved by microwaving the mixture about 2 min. After cooling down the mixture for about 1 minute under the tap water, 2,5µl Safe View agarose gel dye was added, and it was poured to the gel tray with combs in it. After it was solidified, the gel was placed into the gel tank filled with 1X TAE buffer and comb was removed. DNA weigh ladder was loaded into the first well. Samples were mixed with 6X gel loading dye, mixed and loaded to the wells of the gel. The gel was run about 45 minutes at 100V and visualized with Bio-Rad Molecular Imager® Gel Doc™ XR System.

After visualizing, DNA extraction from agarose gel was performed according to the manufacturer's instructions of NucleoSpin® Gel and PCR Clean-up kit.

The cut vector was excised from the agarose gel on the Vilber Lourmart ECX-F20.L UV Transilluminator with the help of a blade. The weight of the gel piece was measured in a tube and for each 100mg of gel, 200µl Buffer NTI was added. The tube was heated to 50ºC for about 5-10min, vortexed in every 1 min until the gel completely dissolved. The sample was loaded into a column in a collection tube. Centrifuged at 11,000 x g for 30sec. The collection tube was emptied, and the column was placed again. 700µl Buffer NT3 was added and centrifuged at 11,000 x g for 30sec to wash the sample. Flow through was discarded and the tube was centrifuged for 1min at 11,000 x g to dry the column. The column was placed into a new clean 1.5ml tube, 30µl Buffer NE was added, incubated for 1min and centrifuged for 1 min at 11,000 x g to elute the DNA.

Ligation

Annealed oligos and digested vector were ligated, 2 control reactions were set up (for each shRNA oligo pairs);

	Control 1;	Control 2;
15,8 µl dH2o	17,3 µl dH2O	16,8 µl dH2O
50ng Vector	50ng Vector	50ng Vector
2 µl T4 ligase buffer	2 µl T4 ligase buffer	2 µl T4 ligase buffer
1 µl annealed oligo pair		
0,5 µl T4 Ligase		0,5 µl T4 Ligase

Ligation performed in room temperature for 2hours.

2.2.1.2. pECPV_gRNA vector construction

Annealing of oligonucleotide pairs

1 µl	Oligo1 (Forward) (100 µM)	Thermocycler parameters:
1 µl	Oligo2 (Reverse) (100 µM)	37^oC 30min
1 µl	10X T4 ligation buffer	95^oC 5min and ramp down to 25^oC at
0,5 µl	T4 PNK	5^oC/min
6,5 µl	H2O	Annealed forward and reverse gRNAs
10 µl	total	were diluted 1/20 ratio.

Digestion of pECPV plasmid

pECPV plasmid (Figure1) was cut with Bsmb1 enzyme and dephosphorylated at room temperature in 1hour in the following reaction mixture;

5 µg   Plasmid

3 µl   FastDigest BsmBI

3 µl   Fast AP (Alkaline phosphatase)

6 µl   10X FastDigest Buffer

X µl   ddH2O

60 µl   total

Gel electrophoresis was done and cut pECPV was purified from the gel using NucleoSpin® Gel and PCR Clean-up kit by following the manufacturer's instructions.

Ligation

Annealed oligos and cut plasmid were ligated in the following ligation reaction;

50ng   BsmBI digested plasmid

1 µl   Diluted oligo duplex

1 µl   T4 ligation buffer

1 µl   T4 ligase

6.35 µl   ddH2O

10 µl   total

Reactions were incubated at RT for 2 hours.

2.2.2. Transformation of bacteria with ligation products

Each ligation product was transformed into the Stbl3 competent bacteria. 15µl of bacteria were added to the ligation reaction tubes, incubated;

On ice 30 minutes,

42ºC water bath 1 minute,

On ice 2 minutes.

1 ml LB media was added to each tube and incubated 37ºC for 1 hour. Centrifuged, supernatants were discarded with keeping little amount of liquid at the bottom of the tube, and pellets were spread to the LB agar plates containing 100 µg/mL Ampicillin. Plates were incubated overnight at 37ºC.

2.2.3. Colony PCR

Colonies formed in the plates were confirmed with colony PCR. Colony PCR protocol;

2 µl   10X Taq Buffer (Mg-free)

1,2 µl   25mM   MgCl2

0,4 µl   10mM dNTPs

0,8 µl   Forward primer (U6 promoter primer) (10µM)

0,8 µl   Reverse primer (Reverse oligo) (10µM)

0,1 µl   Taq Polymerase (5U/µl)

X µl   nuclease-free H2O

20 µl   total + colony picked from the plate with a tip

The tips, after swirling into the PCR tube, were placed into 5 ml LB media with ampicillin (for mini culture).

Thermocycler parameters were as in the table;

Table 12. Colony PCR thermocycler parameters.

Step	Temperature	Time	Number of Cycles
Initial Denaturation	95°C	5 min	1
Denaturation	95°C	30 sec	
Annealing	60°C	30 sec	30
Extension	68°C	30 sec	
Final Extension	68°C	5 min	1

The products were run into 2% agarose gel.

2.2.4. Mini Culture & Plasmid isolation

Verified colonies in the 5ml LB media were grown overnight at 37°C in 225rpm shaker. Plasmids were isolated by using MN NucleoSpin® Plasmid kit. The tube was centrifuged for 10min at 4°C at 3900rpm, the supernatant was discarded. To resuspend the pellet 250µl Buffer A1 was added and pipetted and transferred to a 1,5ml tube. 250µl Buffer A2 was added. The tube was inverted 6-8times and incubated for 5min. After adding 300µl Buffer A3, the tube was inverted 6-8 times until blue samples turn colorless completely. Then, the tube was centrifuged for 5min at 11000 x g at RT. 700µl of the supernatant was loaded onto the column in a collection tube and centrifuged for 1min at 11000 x g. The supernatant was discarded, the column was placed back into the tube. 500ul AW was added to the column and centrifuged for 1min at 11000 x g. 600µl Buffer A4 was added and centrifuged for 1min at 11000 x g. The flow-through was discarded and the column was placed back into the tube. It was centrifuged for 2min at 11000 x g. The column was placed in a 1.5ml microcentrifuge tube. For elution, 50µl Buffer AE was added to the center of the column. It was incubated for 1min at room temperature and centrifuged for 1min at 11000x g.

2.2.5. Lentivirus Production

HEK293T cells were used to package the virus. At t=0h cells were transfected with pECPV-gRNA or pLKO.1-shRNA and helper plasmids by using lipofectamine transfection

reagent. For each pECPV-gRNA vector, Lipofectamine 3000 reagent protocol was performed (Figure 10). For a total of 12μg plasmid, 12μl Lipofectamine 3000 was added to 500μl OptiMEM media. In another tube p3000 DNA mix was prepared with 500μl OptiMEM, 3μg plasmid of interest, 6μg pSPAX2, 3μg pMD2.g, and 24μl p3000. Two tubes were mixed and incubated for 15minutes at room temperature. 80% confluent HEK293T cells in a 100mm dish were washed with 1X PBS and 5ml fresh complete DMEM was added. After incubation 1ml mixture was added to the 100mm dish drop by drop.
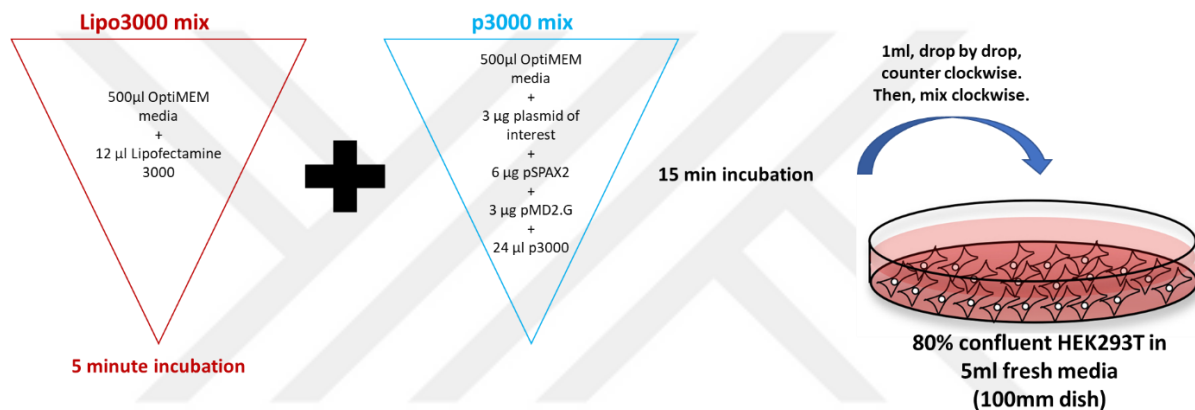
Figure 11. Lentivirus packaging protocol.

At t=16h 4ml complete DMEM was added to the cells. At t=48h the medium of HEK293T cells (10ml) was collected and filtered by using 0,45μm PES membrane filter.

2.2.6. Cell Culture Methods

Maintenance of Cells

Huh7, Hep40, HepG2, Hep3B, Hep3B-TR, PLC/PRF/5, Mahlavu, Sk-Hep1, Focus and Hek293T cell lines were maintained in DMEM high glucose medium supplemented with 10% FBS and 1% Penicillin-Streptomycin (complete DMEM). SNU182, SNU387, SNU398, SNU423, SNU449, SNU475 cell lines were maintained in RPMI medium supplemented with 10% FBS and 1% Penicillin-Streptomycin.

Freezing & Thawing & Subculturing of Cells

For cryopreservation, cells were washed with 1X PBS, TrypLE was added to cover the dish and incubated 3-5min at 37°C. Cells were harvested with growth medium in a falcon tube and centrifuged at 1800 rpm for about 1,5-2min in a tabletop centrifuge. Cell pellet then resuspended in +4°C freezing medium (20% FBS, 72% medium and 8% DMSO) and transferred to cryovial tubes. The vials were kept at -80°C, and liquid nitrogen for long term storage.

For thawing of cells in cryovial, the tube was placed in 37°C water bath. When a small ice was visible, the cells were transferred to a 15ml falcon tube with a 9ml growth medium inside. They were centrifuged at 1800 rpm for about 1,5-2min in a tabletop centrifuge. Cell pellet then resuspended in complete growth medium and transferred in a cell culture dish.

For sub culturing of cells, cells were washed with 1X PBS, TrypLE was added to cover the dish and incubated 3-5min at 37°C. Cells were harvested with growth medium in a falcon tube and centrifuged at 1800 rpm for about 1,5-2min in a tabletop centrifuge. Cell pellet then resuspended in growth medium. 10µl of medium was loaded into the hemocytometer and cells were counted. The cells were seeded in an appropriate number to a dish/plate. If subculturing was just for maintenance, after harvesting the cells, they were split in a proper ratio, considering doubling times of cells.

2.2.7. Virus Infection

The medium containing virus was diluted to 1:20 ratio and 1:1000 polybrene was added. This medium was added onto the cells to be infected. Cells were exposed to virus for 24h. After that they were washed twice with 1X PBS and fresh media was added.

2.2.8. Cell Sorting

Cell sorting was performed by iBG Flow Cytometer Facility. Cells were centrifuged and supernatants were discarded. The pellet was then resuspended in the 1ml FACS buffer. Tubes were filled with media. Samples were kept on the ice and sorted to the tubes containing DMEM with 20% FBS, 2% pen/strep, by FC-1072 Aria III Sorter.

2.2.9. FACS Analysis

Cells were washed with 1X PBS, trypLE was added. After detachment, cells were collected in falcon tubes and centrifuged at 1800rpm for 2min. Supernatant was discarded, and pellet was resuspended in FACS buffer. Cells were transferred into FACS tubes on ice. BD LSRFortessa™ cell analyzer was used to perform FACS (performed by iBG Flow Cytometer Facility) and FlowJo software was used to analyze the results.

2.2.10. Quantitative Real-Time PCR

RNA isolation

RNA isolations were performed using the Macherey-Nagel NucleoSpin® RNA kit. Cells were either scraped or trypsinized, washed with 1X PBS and lysed with 350uL Buffer RA1 and 3,5uL β-mercaptoethanol and vortexed. Lysate was filtered by using violet filter, and filter was discarded. 350uL 70% ethanol was added to the homogenized lysate to adjust RNA binding conditions. The mixture than transferred to the column (blue ring) to bind the RNA. The column was desalted with 350uL MDB (membrane desalting buffer). Column was incubated with DNase reaction mixture, containing 10% rDNase and 90% buffer, at room temperature for 30 minutes. After washing steps with Buffer RAW2 and RA3, RNA was eluted with 60 uL RNase free H2O. Concentrations determined by nano drop measurements.

cDNA synthesis

cDNA synthesis from extracted RNAs were performed by using BIO-RAD iScript™ cDNA Synthesis Kit. Reaction mixture for each reaction was prepared as follows;

Component	Volume (µl)
5x iScript Reaction Mix	4
iScript Reverse Transcriptase	1
Nuclease free water	13
RNA template (1µg)	2
Total	**20**

In a thermal cycler reaction was incubated in following conditions;

5 min at 25°C for priming

20 min at 46°C for reverse transcription

1 min at 95°C for RT inactivation.

The samples were diluted by adding 20ul water (1/2 dilution) and kept at -20°C.

qRT-PCR

qRT-PCR reactions were prepared as follows;

3µl H2O

5µl SYBR green reaction mix

0.4µl Forward and 0.4µ Reverse primer (from 10µM),

2µl (50ng) Template cDNA.

qRT-PCR was performed by using Applied Biosystems® 7500 Fast Real-Time PCR System.

Gene expression calculation

Relative expressions of a gene according to an internal control was calculated based on the Ct values;

Relative expression = 2(Ct Conrol – Ct gene of interest)

2.2.11. Western Blot

Protein isolation

Cells were scraped or trypsinized, washed with 1X PBS and ice-cold RIPA lysis buffer was added onto the pellets. They were incubated for 40 min on ice and vortexed in every 10 min. Cells were centrifuged at full speed, at 4°C for 15 min in a tabletop centrifuge. After centrifugation, the were transferred into new 1.5 ml microcentrifuge tubes and kept on ice.

Bicinchoninic acid (BCA) assay

Serial dilution of albumin standards was prepared as 1000, 500, 250, 125, 62,5, and 31.25 µg/ml with the RIPA buffer. 2 µl of standards and samples were added into 96-well plate as triplicate. Working reagent was prepared by mixing 50X solution A and 1X solution B. 50 µl working reagent was added to each well. Plate was incubated at 37°C for 30 min in the dark and absorbance was measured at 562 nm with Multiskan™ GO Microplate Spectrophotometer. Standard curve was prepared by plotting the average blank-corrected 562 nm measurement for each BSA standard vs. its concentration in µg/mL. The standard curve was used to determine the protein concentration of each sample. The Varioskan software automatically calculates the concentrations.

Protein sample preparation

After equalizing the concentrations, 6x laemmli buffer was added to each sample. 30% β-Mercaptoethanol was added to laemmli buffer prior to use.
The samples were boiled 95°C for 5 min and kept at -80°C.

SDS gel preparation

First separating gel was prepared. Percentage of gel was determined according to size of proteins.

Table 13. 10 ml SDS-PAGE Seperating Gel Recipe.

Components	6%	8%	10%	12%	15%
Protogel (ml)	2	2,7	3,3	4	5
ddH$_2$O (ml)	6,75	6,05	5,3	4,75	3,6
Main gel buffer (ml)	1,25	--→			
10% APS (µl)	50	--→			
TEMED (µl)	10	--→			

The mixture was poured between Western blot glasses. On top of it isopropanol was poured to assure a flat line. After separating gel was polymerized, stacking gel was prepared as below:

Components	2 ml	3 ml	4 ml	5 ml	6 ml	7 ml	8 ml	9 ml	10 ml	11 ml	12 ml
Protogel (ml)	0,25	0,375	0,5	0,625	0,75	0,875	1	1,125	1,25	1,375	1,5
ddH$_2$O (ml)	1,25	1,875	2,5	3,125	3,75	4,375	5	5,625	6,25	6,675	7,5
Protogel stacking buffer pH:6.8 (ml)	0,5	0,75	1	1,25	1,5	1,75	2	2,25	2,5	2,75	3
10% APS (µl)	12,5	18,75	25	31,25	37,5	43,75	50	56,25	62,5	68,75	75
TEMED (µl)	2,5	3,75	5	6,25	7,5	8,75	10	11,25	12,5	13,75	15

Isopropanol was discarded and the stacking gel mixture was poured on top of separating gel and a comb was placed between the glass system. After the gel polymerized the comb was removed. Gel tank was set with 1X running buffer and 20µg of protein sample was loaded to the wells.

Running

Samples were run at 90V until samples leave the stacking gel and then at 120V. Total run was about 1,5 hours.

Transfer of proteins to nitrocellulose membrane

Inside a tank, filled with 1X transfer buffer containing 20% methanol, the gel was removed from the glasses. The transfer sandwich system was prepared. The sandwich clamped tightly. Transfer was performed at 350 mA for 90 min in 1X transfer buffer.

Blocking

Membrane was cut and pieces were placed in a 6-well western blot incubation tray. The membranes were blocked with 5% skim milk powder solved in 1X TBS at RT for 1h.

Blotting

Antibodies were diluted in 1% BSA in an appropriate dilution. Dilutions and for antibodies;

MALT1: 1:250   β-actin: 1:10,000   secondary   antibodies:
α-tubulin: 1:10,000   phospho-Rb: 1:500,   1:10,000

Membranes were incubated with antibodies at $+4^{O}C$ overnight or at room temperature for 2 hours. The membranes were washed with 1X TBS-T for 10min 3 times. They were incubated with secondary antibody, at room temperature for 1 hour.

Imaging

Li-Cor Odyssey Clx imaging system and Image-Studio software were used to image the membranes at 700 and 800 channels. The band signals were analyzed by using Image Studio software.

2.2.12. XTT Viability Assay & IC50 calculation

Biotium XTT Cell Viability Assay Kit was used. 10 ml XTT solution and 50µl activation reagent were mixed. At t=96 40µl of this mixture was added to the wells containing 100µl media + cells. After 3 hours of incubation, the absorbance signals of the plates were measured with the spectrophotometer at a wavelength of 450nm. IC50 calculations were performed with GraphPad Prism software.

2.2.13. Crystal Violet Staining

Media of the cells were discarded; cells were washed with cold 1X PBS. To fix the cells 3,7% formaldehyde was added. Plates were incubated at RT for 20 min or kept at $4^{o}C$ to continue with Crystal violet staining the day after. To prepare 0,5% Crystal Violet staining solution 0.5 g crystal violet powder was dissolved in 80 mL distilled H2O, and 20 mL acetic acid was added. Formaldehyde in the wells were discarded, fixated cells were washed with PBS, then staining solution was added to cover the wells. Plates were incubated for 40min-1h at room temperature. The plates were washed in a stream of tap water and air-dried at room temperature at least for 3 hours. Licor Odyssey CLx Imaging

System and Image Studio software were used to scan the high-resolution images of the plates.

2.2.14. Statistical Analysis

For all statistical analyses GraphPad Prism software was used. To assess the difference of data in two groups Student's t-test was used. Holm-sidak method was used for calculation of statistical significance. When comparing the more than two groups we used two-way ANOVA, and Dunnett's multiple comparisons test was used for calculation of statistical significance.

3. RESULTS

3.1. MALT1 expression in HCC Patient samples

In order to see if there is a difference in MALT1 expression levels between normal liver tissue tumor we performed qRT-PCR with a small cohort of HCC patient cDNA samples, provided by Prof. Dr. Neşe Atabey. This panel includes 2 normal, 1 cirrhosis, and 9 paired patient samples. Pairs have one sample from cirrhosis tissue and one from HCC tissue of the same patient.
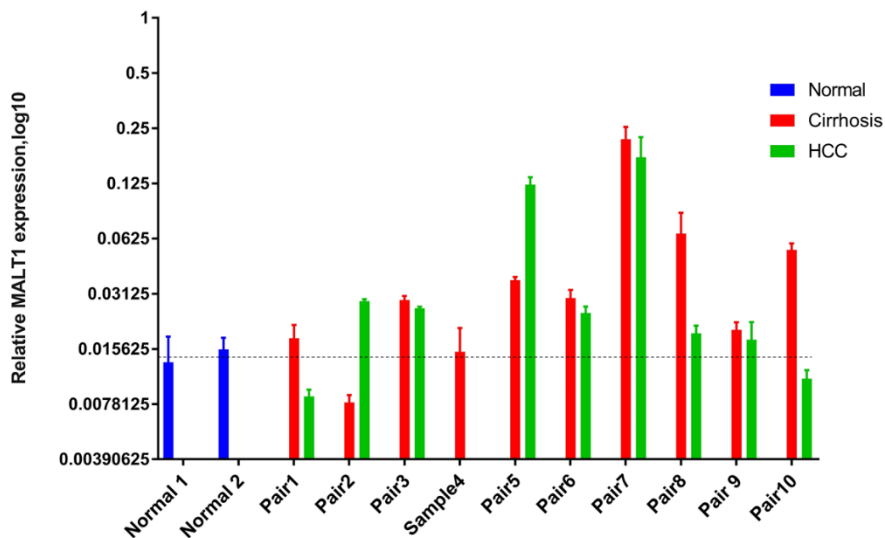

Figure 12. MALT1 expression in patient samples. The dashed line was drawn into the middle value of normal samples.

While nearly all cirrhosis samples have higher expression than that of normal samples, HCC samples have slightly higher MALT1 expression compared to normal tissue. Of note, sample size of normal tissues, in our cohort is very low. More importantly, protein level reflection of these samples could be different than RNA levels. Taken together, these results suggest that MALT1 has an elevated RNA expression in liver disease states, including cirrhosis and HCC. Nonetheless, further studies are required to validate our findings.

3.2. MALT1 expression in HCC cell lines

We then studied the MALT1 expression levels in our 15 HCC cell lines in RNA level. To determine whether the difference in MALT1 expression is correlated with well-differentiated or poorly-differentiated (another grouping method is based on epithelial- or mesenchymal-like gene expression patterns) characteristic, we also used Alpha-fetoprotein (AFP) primers, since AFP expression was shown to discriminate between well- and poorly-differentiated HCC cell lines[43]. qRT-PCR was performed by using Applied Biosystems® 7500 Fast Real-Time PCR System. Relative expressions of MALT1 and AFP according to internal control RPL41 were calculated based on their Ct values (Figure 12A&B). Having shown the RNA levels, we then studied the MALT1 expression at protein level. We performed Western blot analysis in a narrowed sample population (Figure12 C).
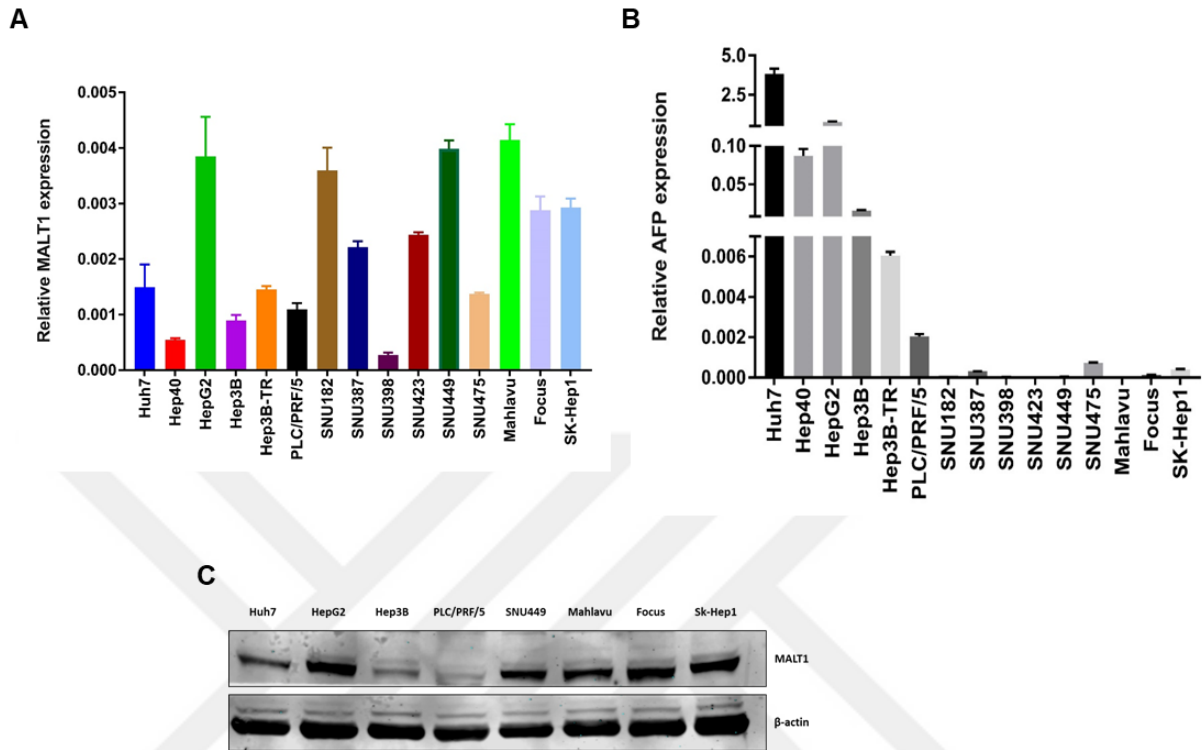
Figure 13. MALT1 expression in HCC cell lines. mRNA levels (A) were corellated with protein levels (C). AFP expression was shown to discriminate between well and poorly differentiated cells (B).

MALT1 is differentially expressed among HCC cell lines. There seems to be no relation between MALT1 expression levels and epithelial or mesenchymal-like characteristic.

3.3. Virus titer determination

Experiments with shRNAs were done in 2 parts; in the first part shSCR and shMALT1-1 were used. shRNA vectors were constructed and verified with sequencing. Lentiviruses containing pLKO-shRNA backbones were produced as described in the methods section. To determine the virus dilution to be used to infect the cells, we set up a dose curve experiment. Six cell lines were plated in 96 well plates (t=0), one cell line in 1 plate. Cell numbers were calculated as if the cells will be confluent in 120 hours.

The cells were infected with lentivirus containing pECPV-shRNA vector construct (t=24h). Dilutions were prepared for each virus; from 1:2 to 1:32 (virus:total media). At

t=48h media of cells were discarded; cells were washed twice with PBS. At t=144 cells were fixed, and Crystal violet staining was performed. Plate images were obtained by using Licor Odyssey CLx Imaging System and Image Studio software.
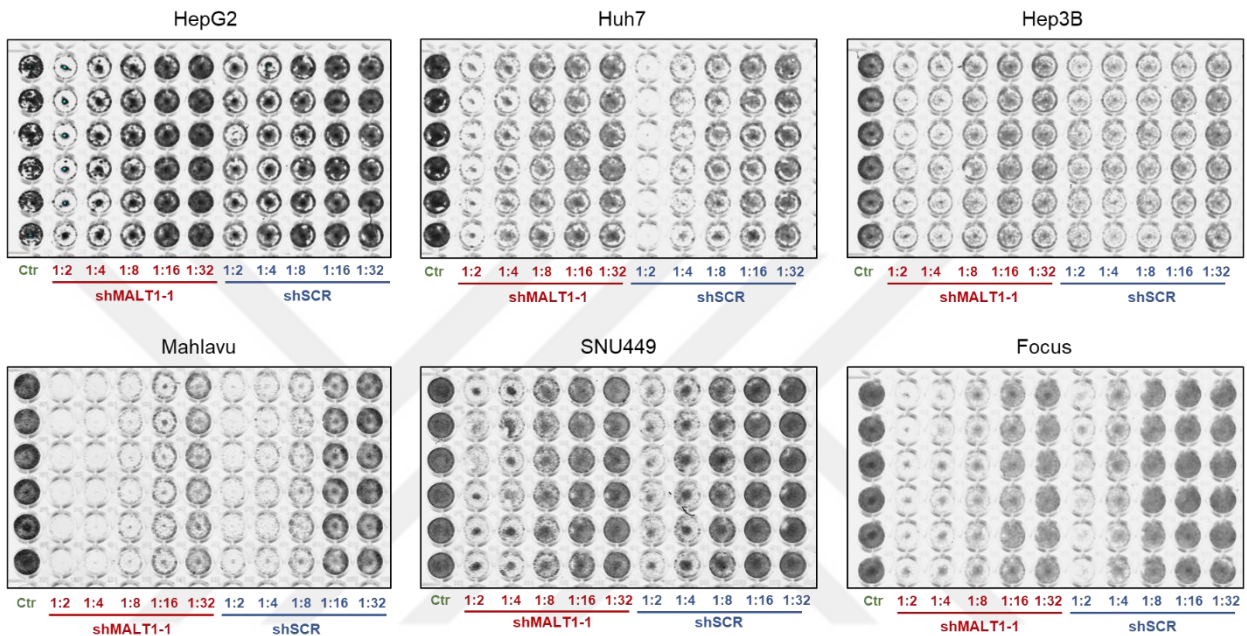

Figure 14. Crystal violet staining images of cells infected with different virus dilutions. Cells were fixed 120h post-infection. N=6 for each virus dilution.

We tried to choose the optimum dilution by comparing shSCR and shMALT1-1 images of same dilution. Because we did not use puromycin to select the infected cells, we tried to saturate the cells with lentivirus without compromising their viability due to non-specific viral toxicity. The dilutions 1:16 and 1:32 did not affect the viability in the shSCR wells, meaning that the lentivirus is not toxic to cells. All in all, 1:16 and 1:32 interval was suitable for our experiments. We, therefore, set the virus dilution to 1:20.

3.4. Knock-down of MALT1 by RNAi system affects survival of HCC cell lines

In the first part, shRNA experiments were done with 2 shRNAs; shSCR and shMALT1-1 (Figure 15). After cloning the second MALT1 shRNA and shRPA3, which is a positive control targeting a cell essential gene, the experiments were collectively repeated with 4 shRNAs (Figure16). For these experiments, cells were plated into 24-well plates

and infected with lentiviruses containing different pLKO.1-shRNA constructs, 3 replicates for each virus. In the first part, where we followed a proof-of-concept design, crystal violet stainings were performed 5 days post-infection, standard for each cell line. In the second part, which was the experimental design, after 1 day post-infection cells were treated with 1 µg/ml puromycin for 3days. Crystal violet was performed after 7-12 days post-infection, based on each cell line's doubling time. High-resolution plate images were obtained by using Li-Cor Odyssey imaging system. Signal intensities of each well were measured with Image Studio software. Most representative well was shown for each shRNA construct (Figure 15&16). Signal intensities of shSCR wells were accepted as 100% and the percentage difference for each well was calculated accordingly.

Figure 15. Knock-down of MALT1 by RNAi system affects survival of HCC cell lines. Cells were infected with either pLKO.1-sh-SCR or pLKO.1-sh-MALT1-1 containing lentivirus, after 120 hours crystal violet staining was performed. Plate images (A) and signal intensities (B) were obtained using Licor Odyssey CLx Imaging System and Image Studio software. n=3 technical replicates. MALT1 mRNA expression levels were decreased by RNAi system (C).

Cells were infected with the same virus dilution and after 3 days post- infection their pellets were collected by scraping, their RNA isolations were performed and MALT1 knock-down levels were showed by qRT-PCR (Figure 14C). For the second part MALT1 knock-down levels were showed by Western Blot (Figure 15C). Cells were infected with 4 shRNA viruses, in the same virus dilution. After 3 days of puromycin selection cells were washed and fresh media was added. At 6 days post-infection cell pellets were collected with trypLE and protein isolations were done. Western Blot performed to show the knock-down efficiencies.

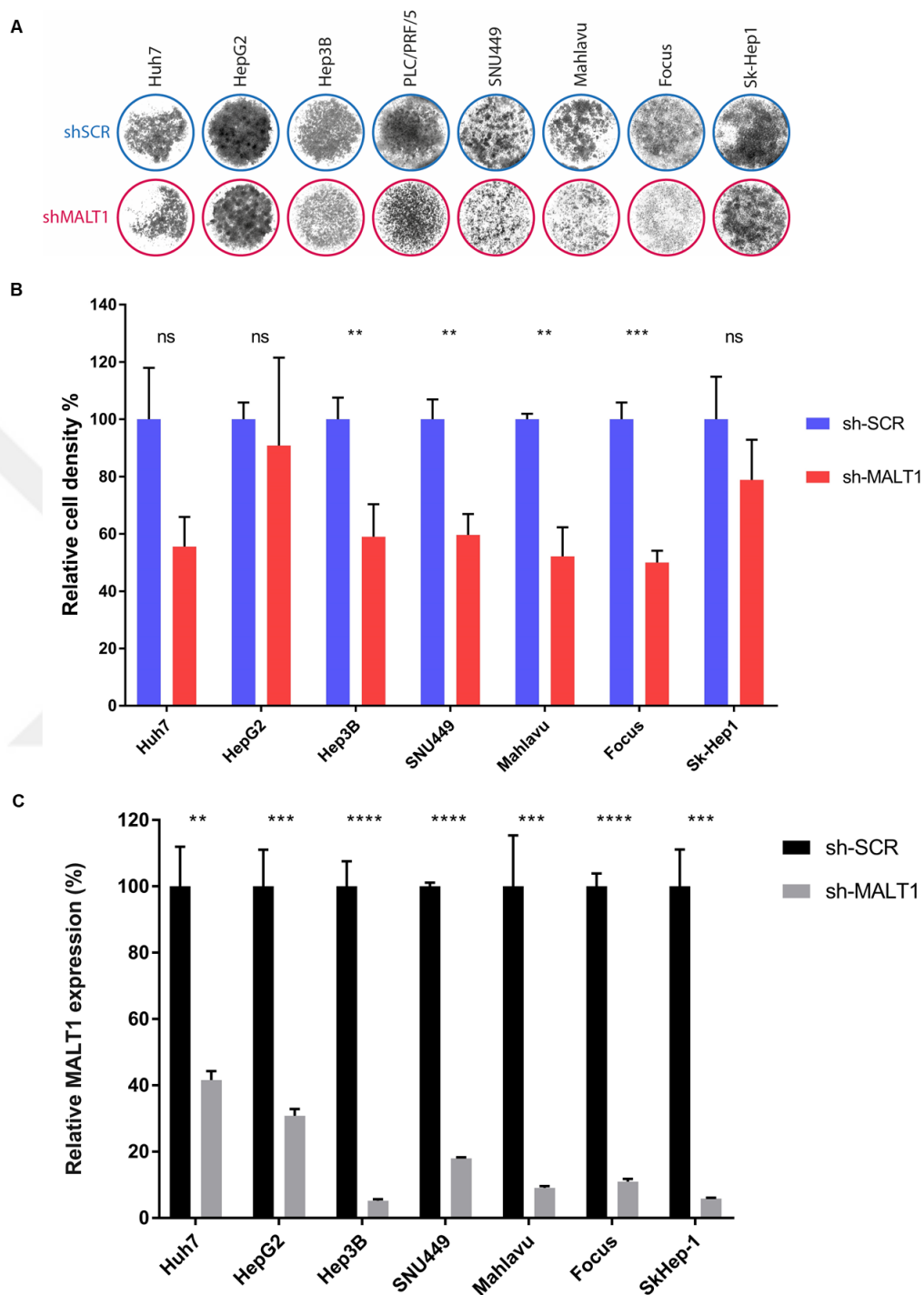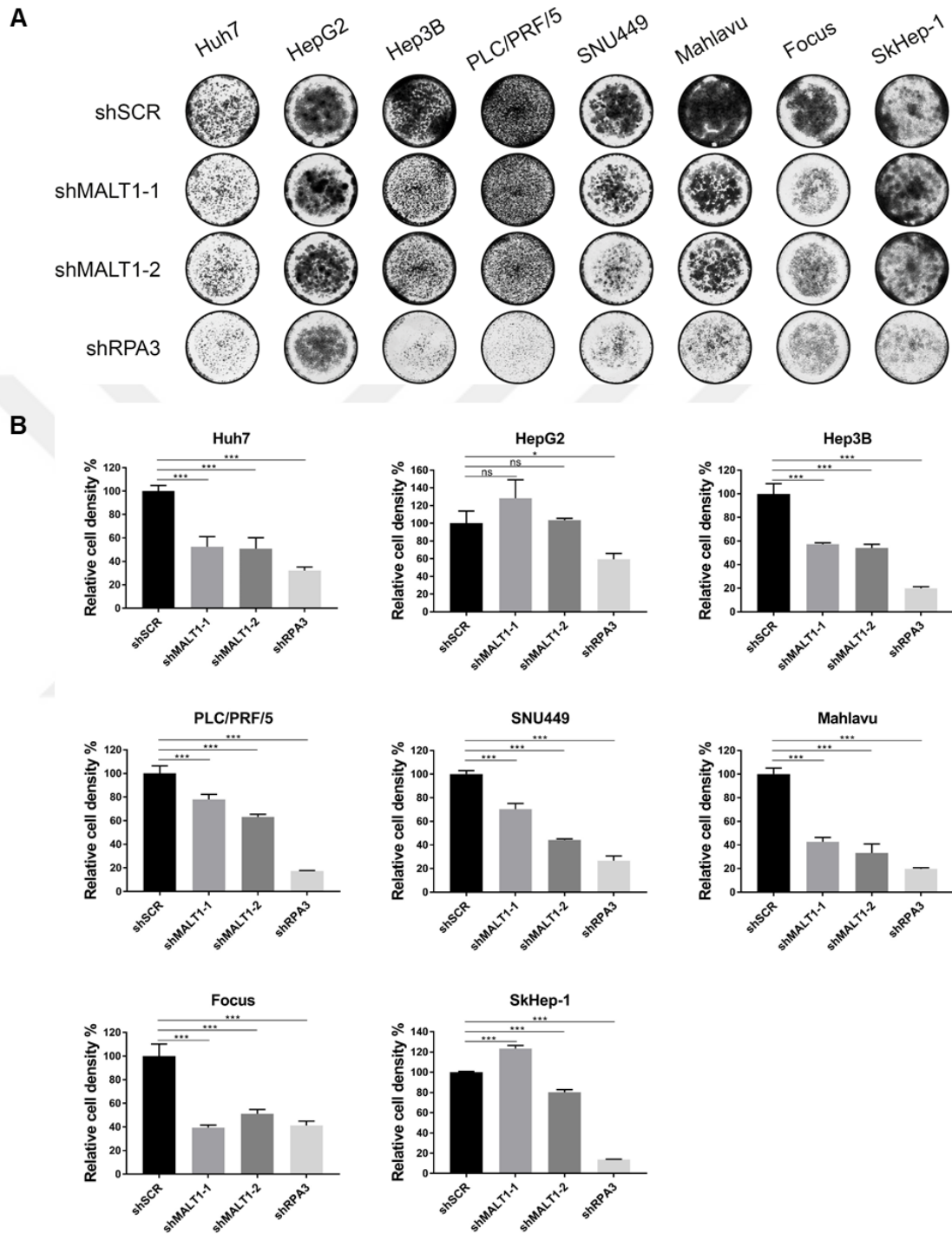*Figure 16. Knock-down of MALT1 by RNAi system affects survival of HCC cell lines. Cells were infected with pLKO.1-sh-SCR or pLKO.1-sh-MALT1-1, pLKO.1-sh-MALT1-2 and pLKO.1-sh-RPA3 containing lentivirus. Puromycin selection was applied. After 7-12 days post- infection crystal violet staining was performed. Plate images (A) and signal intensities (B) were obtained using Licor Odyssey CLx Imaging System and Image Studio software. n=3 technical replicates. Doubling times (h): Huh7:24, HepG2:28, Hep3B:36, PLC/PRF/5:39, SNU449:26, Mahlavu:19, Focus:17, SkHep-1:24.*
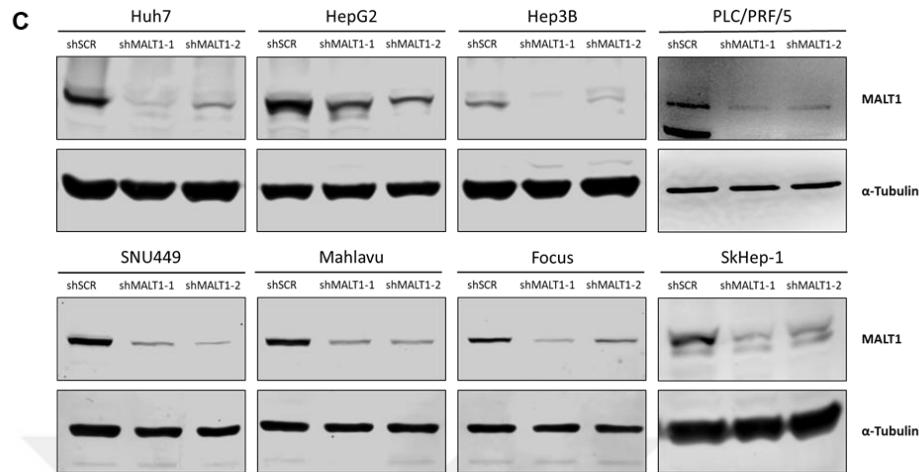
Figure16 contd. Cells were infected with pLKO.1-sh-SCR or pLKO.1-sh-MALT1-1, pLKO.1-sh-MALT1-2 and pLKO.1-sh-RPA3 containing lentivirus. Puromycin selection was applied. After 6 days post-infection WB was performed. MALT1 expression levels were decreased by RNAi system (C). 10% separating gels were used for all blots.

Both in the proof of concept design and experimental design, cell viabilities decreased upon MALT1 knock-down.

3.5. Phospho-Rb levels decreased after MALT1 knockdown

Based on our continuous microscopic observations during the experiment, the decrease in cell number could not be explained with cell death since there were no apoptotic bodies and floating cells. This effect would rather be explained by reduced cell proliferation. We, therefore, checked the levels of phospho-pRb (p-pRb). In cycling cells a tumor suppressor, the retinoblastoma protein (pRb), plays a crucial role in the negative control of the cell cycle. When phosphorylated, it dissociates from E2F which then promotes the transcription of S-phase related genes, allowing cells to progress to S-phase.[44] Cells were infected with relevant shRNA viruses. After 3 days of puromycin selection cells were rinsed with PBS and fresh media was added. 6 days post-infection cell pellets were collected, and protein isolations were done. Western Blot was performed.
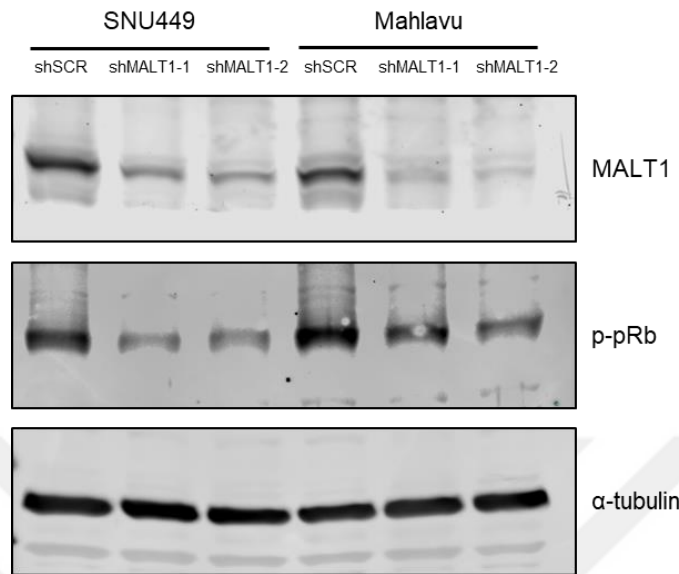
*Figure 17.Western Blot showing phospho-Rb decrease after MALT1 knock-down in SNU449 and Mahlavu cell lines. 8% separating gel was used.*

After an effective MALT1 knock-down, phospho-pRb levels were decreased in SNU449 and Mahlavu cell lines, with both shRNAs.

3.6. IL6 and CCL2 levels were decreased after MALT1 knock-down.

Since MALT1 positively regulates NF-κB pathway, we reasoned that MALT1 knock-down should result in reduced target activity/expression. Hence, we checked the expression of direct targets of the NF-kB pathway after MALT1 knock-down. In the first part of experiments, cells were infected with shSCR or shMALT1-1 viruses. Three days post-infection their pellets were collected, and RNA isolations were performed. qRT-PCR was performed using IL6 primers. IL6, one of the well-established downstream targets of Nf-κB pathway, levels were decreased after MALT1 knockdown.
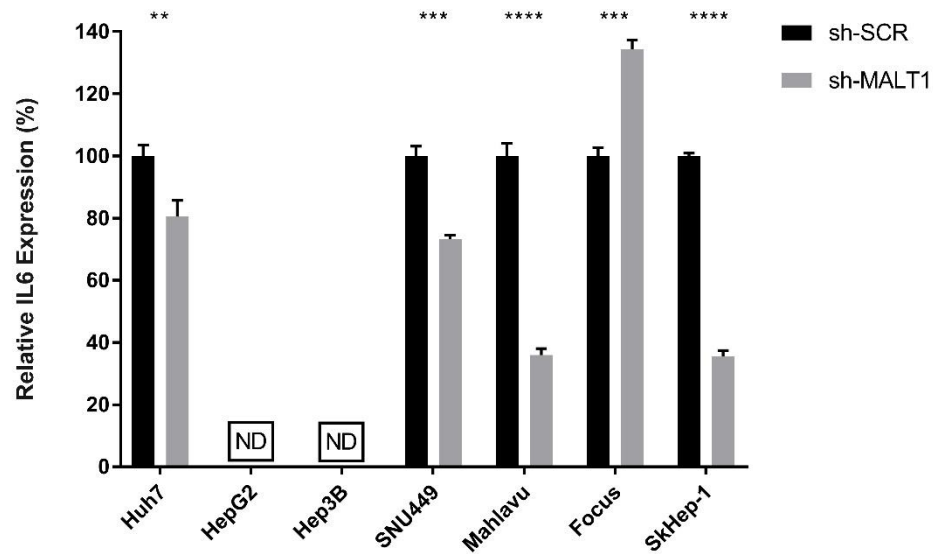
Figure 18. IL-6 levels were decreased after MALT1 knock-down. Cells were infected with either pLKO.1-sh-SCR or pLKO.1-sh-MALT1 containing lentivirus, after 72 hours qRT-PCR was performed. Multiple t-test & Holm-Sidak method for statistical significance. ND: Non-detectable.

Decrease in IL6 levels could be seen in Huh7, SNU449, Mahlavu and SkHep-1 cell lines.

In the second part of experiments, where we used a second MALT1 shRNA, cells were infected and selected with puromycin for 3 days. After 6 days post-infection their pellets were collected, and RNA isolations were performed. qRT-PCR was performed using IL6 and CCL2 primers. IL6 and CCL2 levels, both are downstream targets of NF-κB pathway, were decreased after MALT1 knockdown.
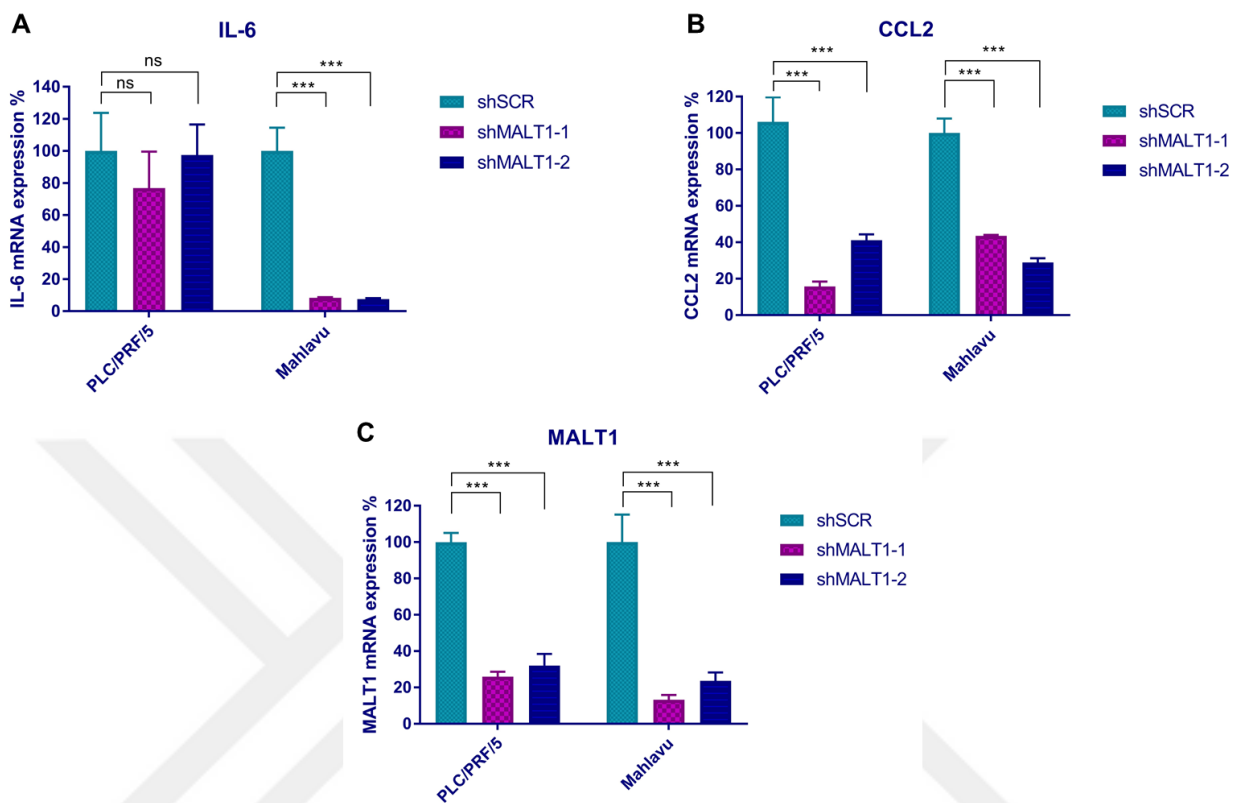
Figure 19. IL-6 (A) and CCL-2 (B) levels were decreased after MALT1 knockdown (C).

After showing the effects of MALT1 depletion by RNAi system, we wanted to strengthen our results by depleting MALT1 via CRISPR-Cas9 system.

3.7. Depletion of MALT1 by CRISPR-Cas9 system

Four different MALT1 gRNAs, gRen and gRPA3 were cloned into pECPV backbone. Lentiviruses were produced using gRNA vectors and helper vectors. First, to determine the gRNA efficiency, HepG2 cells infected with lentivirus containing 4 different pECPV-gRNA backbone; g258, g259, g268, g272 and a control gRNA; gRen. with a 1:20 virus dilution. After 48hours post-infection, bulk sorting was performed for each infected cell group. The highest 30% percentages were sorted and plated in 6cm dishes with 20% FBS containing medium. After 120hours from sorting, cells were collected with scraper on ice, protein isolation and western blot was performed. The maximum protein depletion was achieved by using g259.
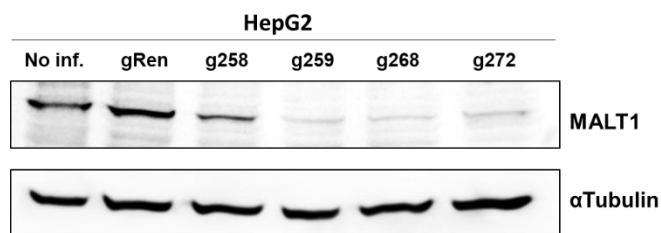
Figure 20. gRNA verification by western blot. Lentivirus system was used to infect HepG2 cells with different viruses containing pECPV-gRNA backbone. Western Blot validation of MALT1 depletion in cells 5 days post-infection.

3.8. Competition Assay

In order to track if the ratio of viable infected cells in a population decreases over time, we set up a competition assay experiment. To perform competition assay we chose two most efficient gRNAs; g259 and g268. Besides these, we use one negative and one positive control gRNAs; gRen and gRPA3. Cells were infected with pECPV-gRNA viruses, gRen, g259, g268, gRPA3. Two days post-infection, at t=0d FACS analysis was done. 1/10 of the cells was collected from 6cm dishes, centrifuged and pellets were resuspended in 100ul FACS buffer. Cells were transferred into FACS tubes on ice. The rest of the cells were passaged to continue culturing. BD LSRFortessa™ cell analyzer was used to perform FACS (performed by iBG Flow Cytometer Facility) and FlowJo software was used to analyze the Venus positive cell percentage among each group. At t=4d, t=8d and t=12d FACS analysis was repeated.
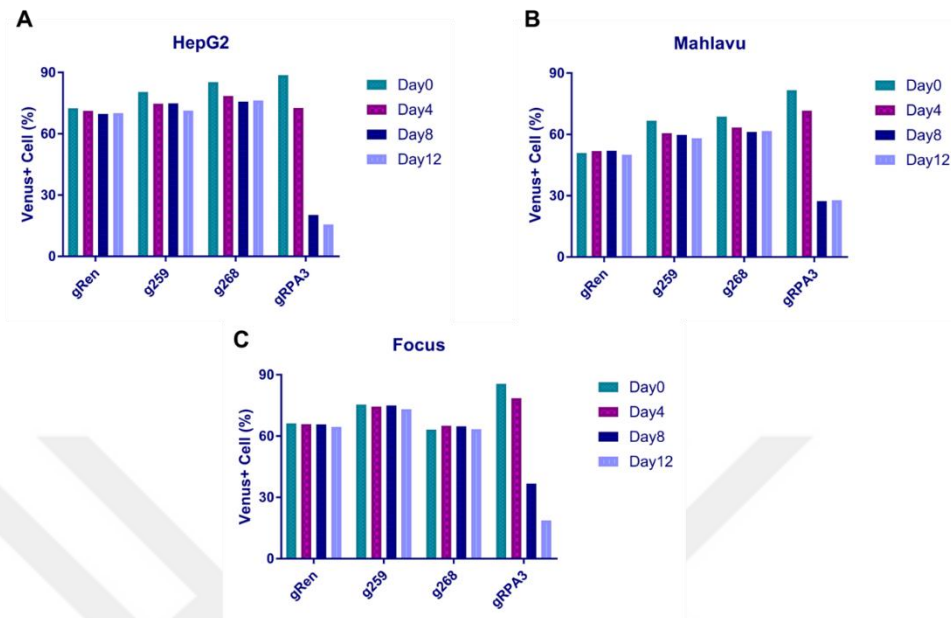
Figure 21. Competition assay. Graphs showing the Venus+ cell percentage at each time point in an infected cell group. Competition assay was performed with HepG2 (A), Mahlavu (B) and Focus (C) cell lines.

The Venus positivity in gRen infected group in each cell line stayed unchanged, from day 0 to day 12. The Venus positivity in gRPA3 infected group decreased dramatically since RPA3.44 is a vital gene whose protein functions in DNA replication as well as DNA-damage repair processes. However, there is not any significant change in Venus positive cell percentage in MALT1 gRNAs infected cells in all 3 cell lines (Figure). The results of this experiment were discussed extensively in discussion part.

3.9. MALT1 inhibitor MI-2 decreases viability of HCC cell lines.

Finally, we aimed to show the effects of MALT1 depletion via another strategy, by using a small molecule inhibitor. MI-2 was used to inhibit MALT1 in cells . In order to study the effect of Malt1 inhibition by MI-2, Each cell line was plated in a 96-well plate. Cell numbers for each well were calculated in a way that they would be 90% confluent at the end of the experiment, namely 120h post-plating. At t=0 cells were plated in 50 µl media to each well. MALT1 inhibitor was prepared from powder. To obtain a final concentration of 100mM stock solution it was dissolved in 219.433 µl DMSO. Inhibitor concentrations to be applied to the cells were calculated accordingly and prepared in falcon tubes from the

main stock. 200µM 2640µl inhibitor was prepared from stock with DMEM media, then with ½ serial dilutions 9 concentrations (given below) were prepared;

200 µM, 100 µM, 50 µM, 25µM, 12.5 µM, 6.25 µM, 3.125 µM, 1.5625 µM, 0.78125 µM.

At t=24 50 µL of MALT1 inhibitor was added to the wells containing cells + 50 µL media. The final concentrations and the plate design were as following;

	0 µM	100 µM	50µM	25µM	12.5µM	6.25µM	3.125µM	1.56µM	0.78µM	0.39µM	
	0 µM	100 µM	50µM	25µM	12.5µM	6.25µM	3.125µM	1.56µM	0.78µM	0.39µM	
	0 µM	100 µM	50µM	25µM	12.5µM	6.25µM	3.125µM	1.56µM	0.78µM	0.39µM	
	0 µM	100 µM	50µM	25µM	12.5µM	6.25µM	3.125µM	1.56µM	0.78µM	0.39µM	
	0 µM	100 µM	50µM	25µM	12.5µM	6.25µM	3.125µM	1.56µM	0.78µM	0.39µM	
	0 µM	100 µM	50µM	25µM	12.5µM	6.25µM	3.125µM	1.56µM	0.78µM	0.39µM	

At t=96 XTT assay was performed and IC50 calculations were performed with GraphPad Prism software.
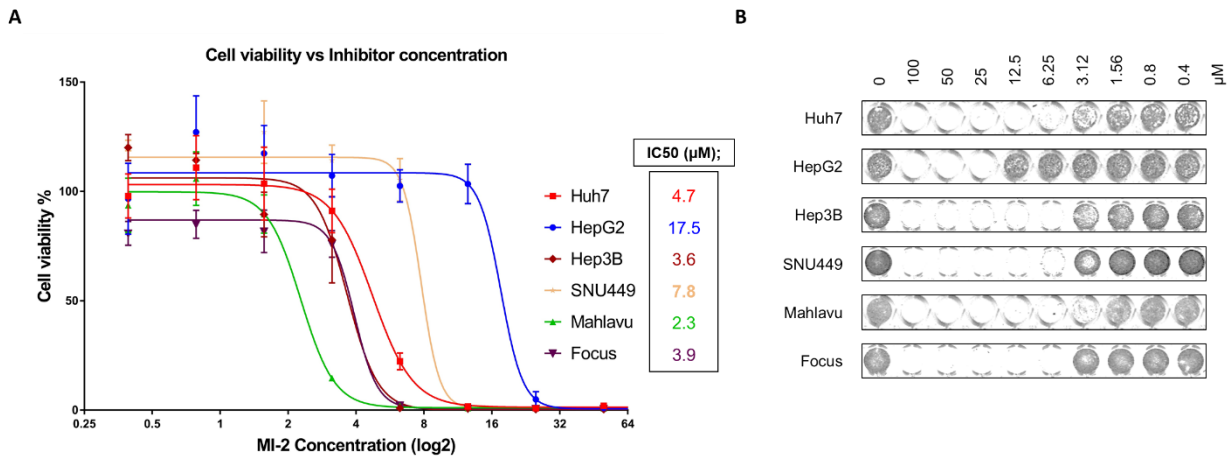
Figure 22. (A) MALT1 inhibitor sensitivity differs among cells according to XTT viability assay. (B) Viable cells were fixed, stained with Crystal Violet and visualized after MI-2 treatment of varying concentrations. n=6 technical replicates and at least 2 biological replicates.

IC50 values differs among cells. HepG2 has the highest value of IC50, in consistent with the shRNA results. Mahlavu seemed to be the most sensitive cell line to MALT1 deprivation.

4. <u>DISCUSSION</u>

Hepatocellular carcinoma is a leading cause of cancer related deaths worldwide. During hepatocarcinogenesis a number of molecular pathways are altered including WNT-β-catenin, phosphoinositol-3-kinase/Akt, hedgehog, p53, NF-κB and c-Met pathways. In 80-90% of the cases, HCC develops from cirrhosis, the main causes of which are HCV and HBV infections. Both HBV and HCV can promote hepatocarcinogenesis by regulating several pathways including WNT-β-catenin, p53 and Nf-κB and Raf/MAPK pathways. Other risk factors include alcohol consumption, nonalcoholic fatty liver disease, nonalcoholic steatohepatitis, obesity and aflatoxin B1 exposure.

Systemic treatments that target Tyrosine Kinases (TKs) and Cyclin-Dependent Kinases are offered to advanced stage HCC patients. Currently Sorafenib, Regorafenib, Lenvatinib and Cabozatinib are being used for treatment however patients develop resistance and ongoing clinical trials have not shown a superior effect against current drugs. Immune checkpoint inhibitors, which are all in clinical trials, are another treatment strategy and currently there are no approved checkpoint inhibitor for HCC.

NF-κB pathway which controls the expression of number of genes related to survival, proliferation, apoptosis, immune response etc., is one of the dysregulated pathways in HCC. Both HBV and HCV infections could lead to activation of NF-κB pathway in primary hepatocytes. MALT1 is a signaling component of NF-κB pathway and it acts as a both cytosolic scaffolding protein for the pathway activation and as a protease for the pathway regulation by cleaving negative regulators of NF-κB pathway. Besides in immune cells, MALT1 importance in cell survival has been shown in several tumors as lung cancer, oral squamous cell carcinoma and ovarian cancer. MALT1 dependent NF-κB pathway activation in different cell types is a promising area for future research. Also having a minor functional and structural homology to other proteins, MALT1 has an advantage as a therapeutic target.

Our aim in this study was to investigate the role of MALT1 paracaspase in hepatocellular carcinoma cell survival. To achieve this goal, we depleted MALT1 in HCC

cells via 3 methods; RNAi system, CRISPR-Cas9 system and small molecule inhibitor and measure the cell viability with different assays.

As a first step we checked the MALT1 expression levels in a cohort of patient cDNA samples. Compared to normal samples, while nearly all cirrhosis samples have higher expressions, HCC samples have slightly higher MALT1 expressions. Even though the sample cohort is small, and the number of normal samples are very low, we could say that MALT1 has an elevated RNA expression in liver disease states, including cirrhosis and HCC. Besides, RNA levels are not directly correlated with protein levels therefore further studies are required to validate our findings.

We then studied the MALT1 expression levels in our 15 HCC cell lines in RNA level. At the same time, we validated their well-differentiated or poorly differentiated (or epithelial or mesenchymal-like) characteristics by checking Alpha-fetoprotein (AFP) levels. We saw that MALT1 is differentially expressed among HCC cell lines and there seems to be no relation between MALT1 expression levels and epithelial or mesenchymal-like characteristics. We then selected 8 cell lines for further experiments, 4 from well-differentiated and 4 from poorly-differentiated cells and checked the protein levels of MALT1. Protein levels, shown by western blot, are correlated with RNA levels.

For our first strategy to deplete MALT1, we constructed shRNA vectors using pLKO.1 backbone. We used lentivirus system to provide continuous expression of shRNAs. In our first proof of concept design, we used shSCR as a negative control and one MALT1 shRNA. To determine the virus dilution to be used to infect the cells, we set up a dose curve experiment with 6 cell lines. The cells were infected with lentivirus containing pLKO.1-shRNA vector construct in dilutions from 1:2 to 1:32 (virus:total media). Cells were fixed and stained with crystal violet 5 days post-infection. Since we aimed to observe the acute effect of MALT1 depletion in survival, we did not apply puromycin selection, and therefore we tried to saturate the cells with lentivirus. Here, we also wanted to avoid non-specific viral toxicity while choosing the titer. For most of the cells, the dilutions 1:16 and 1:32 did not affect the viability in the shSCR wells, meaning that the lentivirus is not toxic to cells. However, for Hep3B and Huh7, even in 1:32 dilution, cell

viability was decreased compared to non-infected wells. This could be the toxic effect of polybrene, which is used in 1:1000 ratio while infecting the cells. Since we aim to compare the difference of cell densities between shSCR and shMALT1 wells that were infected with the same virus dilution, we chose the highest dilutions in which the viability differences between shSCR and shMALT1 were significant and independent of viral toxicity. All in all, 1:16 and 1:32 interval was suitable for our experiments. We, therefore, set the virus dilution to 1:20. We then used this virus titer to infect the panel of 7 HCC cell lines, Huh7, HepG2, Hep3B, SNU449, Mahlavu, Focus and Sk-Hep1. Of note, we also used PLC/PRF/5 in the first part of the experiments, however we had a suspicion about the cell line's characteristics, since over time in the culture it failed to show the PLC/PRF/5 typical features, as cell shape and doubling time, therefore we discarded its results. Crystal violet stainings were performed, in 24 well plates, 5 days post-infection, standard for each cell line. By using same conditions, we infected the cells and checked MALT1 knock-down in three days. Even in three days the knock-down efficiencies were very high, reaching up to 90% (Figure 14C). In 5 days, most of the cells showed decreased proliferation (Figure 14A&B). After seeing the effect of MALT1 depletion, we set up an experimental design and used an additional MALT1 shRNA and a positive control shRNA for RPA3 gene which is essential for cell survival. In the initial experiments (results not shown) the antiproliferative effects of RPA3 knock-down were detected at least after 7 days post-infection. Based on these observations we aimed to avoid the representation of non-infected cell population (if present) in the long-term experimental set up, we applied puromycin selection for 3 days. Nonetheless, the number of un-infected cells were negligible. We fixed and stained the cells 7-12 days post-infection based on each cell line's doubling time. Some cells, like PLC/PRF/5, showed the depletion effect later than others. We believed that this could be explained in part, due to higher doubling time, hence comparably slower proliferation rate. We also observed the cells in shRPA3 wells and waited to see the RPA3 depletion effect, apoptosis and decreased proliferation, before finishing the experiment. We saw that the viabilities of HCC cell lines, except HepG2 and SkHep-1, decreased dramatically, upon MALT1 knock-down (Figure 15A). To check the knock-down efficiencies we performed WB 6 days post-infection. MALT1 protein levels

54

were successfully reduced by RNAi system (Figure 15C). In this experiment during which we microscopically followed the cell proliferation, we were not able to observe formation of apoptotic bodies and/or floating cells, we reasoned that the decrease in cell number could not be directly explained with cell death. This effect would rather be explained by reduced cell proliferation. We, therefore, checked the levels of phospho-pRb (p-pRb) in 2 cell lines, namely SNU449 and Mahlavu. Of note, in cycling cells the retinoblastoma protein (pRb), a tumor suppressor, plays a pivotal role in the negative control of the cell cycle. When phosphorylated, it dissociates from E2F which then promotes the transcription of S-phase related genes, allowing cells to progress to S-phase. We saw that phospho-pRb levels were significantly decreased in SNU449 and Mahlavu cell lines following MALT1 knock-down with both shRNAs (Figure 16). Taken together, this result suggests that MALT1 depletion could reduce cell proliferation by leading to inhibition of S-phase entry.

MALT1 has central roles in NF-κB pathway as a positive regulator, therefore we believed that MALT1 knock-down should result in reduced target activity/expression. Therefore, we checked the expression of direct targets of the NF-kB pathway after MALT1 knock-down. IL-6 levels were decreased after MALT1 knock-down in both proof-of-concept design and experimental design (Figure 17, Figure 18A). Unfortunately, we could not see the expected decrease in PLC/PRF/5 cells (Figure 18A), suggesting that IL-6 expression in this cell line could be regulated via NF-kB pathway-independent mechanisms which of course requires further investigation. Nevertheless, we saw that CCL2 levels were decreased in PLC/PRF/5 and Mahlavu cell lines (Figure 18B) after an effective MALT1 knock-down (Figure 18C). The decrease in IL-6 as well as CCL2 levels confirms that MALT1 depletion leads to NF-kB pathway inactivation in select HCC cell lines.

One of the targets of MALT1 is CYLD, the protein cylindromatosis, a deubiquitinating enzyme. It is known that CYLD enzyme is a negative regulator of several pathways such as NF-κB, WNT-β-catenin and JNK pathways[45]. Since MALT1 degrades CYLD, MALT1 depletion could result in the downregulation of these pathways and decreased expression

of their target genes. NF-κB and JNK pathways can regulate the transcription of cytokines such as IL1 and IL6 in the liver[46]. Therefore, the decrease in the CCL2 and IL6 levels in 2 HCC cell lines PLC/PRF/5 and Mahlavu could be a collective effect of the downregulation of these pathways, which of course requires further investigation.

Our second strategy was to deplete MALT1 with CRISPR-Cas9 system in order to confirm and strengthen our results. After cloning four different MALT1 gRNAs, gRen and gRPA3 into the pECPV backbone, lentivirus system was used to infect the cells. First gRNA efficiency was measured in sorted HepG2 cells by western blot (Figure19). We chose two most efficient gRNAs; g259 and g268 to set up a competition assay, we also used gRen and gRPA3 as negative and positive controls respectively. Here, we aimed to tract the viable infected cells in a population over time. We infected 3 cell lines, HepG2, Mahlavu and Focus with 4 gRNA containing viruses and measured the Venus positivity once every 4 days (Figure 20). In gRen groups we expected the percentage of infected populations to stay unchanged from day0 to day12, since gRen does not target anywhere in the human genome. In gRPA3 group, the Venus positivity decreased dramatically in all three cell lines since the RPA3 gene is essential for the cells and targeting RPA3 is lethal. From our shRNA results, we deduced that MALT1 depletion reduced HCC cell survival, except in HepG2, therefore we assumed that the Venus positivity ratio in MALT1 targeted cell populations will decrease over time. However, we could not see any decrease in Venus positive cell percentage in those groups. This could be explained in several ways. Firstly, our gRNA design could be faulty and CRISPR system could not work in Mahlavu and Focus cell lines. According to a study done in 2015, gRNA target sites that have multiple PAMs can decrease the efficiency of Cas9 cleavage.[47] All our gRNAs have more than 1 PAM sites in them therefore this could interfere with the Cas9 cleavage of MALT1 gene. Another reason could be reduced expression of certain cytokines such as IL-6 and CCL2 from the MALT1 depleted cell population. In our microscopic observations, before each flow cytometry analysis, we observed that the cell number in all populations, except gRen group, decreased significantly. Considering the high infection rate of the cells, if the MALT1 depletion in infected cell populations caused reduced cytokine release, non-

infected cell viability could also decrease in a cell-nonautonomous manner. We are planning to repeat the competition assay experiments either with a new set of gRNAs or with a new backbone where we will use shRNAs.

In our last strategy, we use small molecule inhibitor, MI-2, to deplete MALT1 in HCC cell lines. We measure cell viability by XTT assay. The results showed that the IC50 values differs among HCC cells. HepG2 is the most resistant one to deprivation, in consistent with the shRNA results. Mahlavu seemed to be the most sensitive cell line to MALT1 deprivation. This experiment shows that the survival of the HCC cell lines can be decreased by using small molecule inhibitor of MALT1.

5. <u>CONCLUSION AND FUTURE PERSPECTIVES</u>

We showed that MALT1 depletion, and therewithal NF-kB pathway inactivation, could lead reduced cell survival in HCC cell lines. This effect could be explained by reduced cell proliferation and inhibition of S-phase entry, according to decreased p-pRb levels. Both RNAi system and small molecule inhibitor produced the same result however, CRISPR-Cas9 system was somehow not functional. We will repeat the competition assay with a new set of gRNAs or change our strategy and use a new backbone where we will use shRNAs. As a next step, will show the changes in NF-kB pathway proteins after MALT1 knock-down. We are also planning to perform cell cycle analysis in a narrowed set of HCC cell lines after infection with shRNA viruses. And if the results will be promising, we will check cell cycle proteins. We are also planning to set up a rescue experiment, where we will re-express MALT1 in knocked-down cells to show that the decrease in cell proliferation is a specific effect of MALT1 deprivation. All in all, we will broaden our understanding of how MALT1 decreases cell survival in HCC cell lines.

6. <u>REFERENCES</u>

1. Bray, F. *et al.* Global cancer statistics 2018: GLOBOCAN estimates of incidence and mortality worldwide for 36 cancers in 185 countries. *CA. Cancer J. Clin.* **68**, 394–424 (2018).

2. Llovet, J. M. *et al.* Hepatocellular carcinoma. *Nat. Rev. Dis. Primer* **2**, 16018 (2016).

3. Sanyal, A. J., Yoon, S. K. & Lencioni, R. The Etiology of Hepatocellular Carcinoma and Consequences for Treatment. *The Oncologist* **15**, 14–22 (2010).

4. Nault, J. C. *et al.* High frequency of telomerase reverse-transcriptase promoter somatic mutations in hepatocellular carcinoma and preneoplastic lesions. *Nat. Commun.* **4**, 2218 (2013).

5. Ghouri, Y., Mian, I. & Rowe, J. Review of hepatocellular carcinoma: Epidemiology, etiology, and carcinogenesis. *J. Carcinog.* **16**, 1 (2017).

6. Szabó, E., Páska, C., Novák, P. K., Schaff, Z. & Kiss, A. Similarities and differences in hepatitis B and C virus induced hepatocarcinogenesis. *Pathol. Oncol. Res.* **10**, 5–11 (2004).

7. Xu, W., Yu, J. & Wong, V. W.-S. Mechanism and prediction of HCC development in HBV infection. *Best Pract. Res. Clin. Gastroenterol.* **31**, 291–298 (2017).

8. Geng, M. Molecular mechanism of hepatitis B virus X protein function in hepatocarcinogenesis. *World J. Gastroenterol.* **21**, 10732 (2015).

9. Jeong, S. W., Jang, J. Y. & Chung, R. T. Hepatitis C virus and hepatocarcinogenesis. *Clin. Mol. Hepatol.* **18**, 347 (2012).

10. Jindal, A., Thadi, A. & Shailubhai, K. Hepatocellular Carcinoma: Etiology and Current and Future Drugs. *J. Clin. Exp. Hepatol.* **9**, 221–232 (2019).

11.   Medavaram, S. & Zhang, Y. Emerging therapies in advanced hepatocellular carcinoma. *Exp. Hematol. Oncol.* **7**, 17 (2018).

12.   Chen, S., Cao, Q., Wen, W. & Wang, H. Targeted therapy for hepatocellular carcinoma: Challenges and opportunities. *Cancer Lett.* **460**, 1–9 (2019).

13.   Personeni, N., Pressiani, T. & Rimassa, L. Lenvatinib for the treatment of unresectable hepatocellular carcinoma: evidence to date. *J. Hepatocell. Carcinoma* **Volume 6**, 31–39 (2019).

14.   Pinter, M. & Peck-Radosavljevic, M. Review article: systemic treatment of hepatocellular carcinoma. *Aliment. Pharmacol. Ther.* **48**, 598–609 (2018).

15.   Llovet, J. M., Montal, R., Sia, D. & Finn, R. S. Molecular therapies and precision medicine for hepatocellular carcinoma. *Nat. Rev. Clin. Oncol.* **15**, 599–616 (2018).

16.   Marquardt, J. U., Saborowski, A., Czauderna, C. & Vogel, A. The Changing Landscape of Systemic Treatment of Advanced Hepatocellular Carcinoma: New Targeted Agents and Immunotherapies. *Target. Oncol.* **14**, 115–123 (2019).

17.   Immune Checkpoint Inhibitors in Hepatocellular Carcinoma: Opportunities and Challenges. *The Oncologist* **24**, S3–S10 (2019).

18.   Baud, V. & Karin, M. Is NF-κB a good target for cancer therapy? Hopes and pitfalls. *Nat. Rev. Drug Discov.* **8**, 33–40 (2009).

19.   Shokri, S., Mahmoudvand, S., Taherkhani, R., Farshadpour, F. & Jalalian, F. A. Complexity on modulation of NF-κB pathways by hepatitis B and C: A double-edged sword in hepatocarcinogenesis. *J. Cell. Physiol.* **234**, 14734–14742 (2019).

20.   Kim, H. R., Lee, S. H. & Jung, G. The hepatitis B viral X protein activates NF-κB signaling pathway through the up-regulation of TBK1. *FEBS Lett.* **584**, 525–530 (2010).

21.   Arsura, M. & Cavin, L. G. Nuclear factor-κB and liver carcinogenesis. *Cancer Lett.* **229**, 157–169 (2005).

22.   Robinson, S. M. & Mann, D. A. Role of nuclear factor κB in liver health and disease. *Clin. Sci.* **118**, 691–705 (2010).

23.   Sun, S.-C. The non-canonical NF-κB pathway in immunity and inflammation. *Nat. Rev. Immunol.* **17**, 545–558 (2017).

24.   Hayden, M. S. & Ghosh, S. Signaling to NF-kappaB. *Genes Dev.* **18**, 2195–2224 (2004).

25.   Lin, Y., Bai, L., Chen, W. & Xu, S. The NF-κB activation pathways, emerging molecular targets for cancer prevention and therapy. *Expert Opin. Ther. Targets* **14**, 45–55 (2010).

26.   Zhang, Q., Lenardo, M. J. & Baltimore, D. 30 Years of NF-κB: A Blossoming of Relevance to Human Pathobiology. *Cell* **168**, 37–57 (2017).

27.   Moynagh, P. N. The NF- B pathway. *J. Cell Sci.* **118**, 4589–4592 (2005).

28.   Rosebeck, S., Rehman, A. O., Lucas, P. C. & McAllister-Lucas, L. M. From MALT lymphoma to the CBM signalosome: Three decades of discovery. *Cell Cycle* **10**, 2485–2496 (2011).

29.   Jaworski, M. & Thome, M. The paracaspase MALT1: biological function and potential for therapeutic inhibition. *Cell. Mol. Life Sci.* **73**, 459–473 (2016).

30. Israël, L. & Bornancin, F. Ways and waves of MALT1 paracaspase activation. *Cell. Mol. Immunol.* **15**, 8–11 (2018).

31. Juilland, M. & Thome, M. Holding All the CARDs: How MALT1 Controls CARMA/CARD-Dependent Signaling. *Front. Immunol.* **9**, 1927 (2018).

32. Lan, P. *et al.* TNF superfamily receptor OX40 triggers invariant NKT cell pyroptosis and liver injury. *J. Clin. Invest.* **127**, 2222–2234

33. Bonsignore, L. *et al.* A role for MALT1 activity in Kaposi's sarcoma-associated herpes virus latency and growth of primary effusion lymphoma. *Leukemia* **31**, 614–624 (2017).

34. Afonina, I. S., Elton, L., Carpentier, I. & Beyaert, R. MALT1 - a universal soldier: multiple strategies to ensure NF-κB activation and target gene expression. *FEBS J.* **282**, 3286–3297 (2015).

35. Pan, D. *et al.* MALT1 is required for EGFR-induced NF-κB activation and contributes to EGFR-driven lung cancer progression. *Oncogene* **35**, 919–928 (2016).

36. Rehman, A. O. & Wang, C. CXCL12/SDF-1α Activates NF-κB and Promotes Oral Cancer Invasion through the Carma3/Bcl10/Malt1 Complex. *Int. J. Oral Sci.* **1**, 105–118 (2009).

37. Mahanivong, C. *et al.* Protein kinase Cα-CARMA3 signaling axis links Ras to NF-κB for lysophosphatidic acid-induced urokinase plasminogen activator expression in ovarian cancer cells. *Oncogene* **27**, 1273–1280 (2008).

38. Demeyer, A., Staal, J. & Beyaert, R. Targeting MALT1 Proteolytic Activity in Immunity, Inflammation and Disease: Good or Bad? *Trends Mol. Med.* **22**, 135–150 (2016).

39.   Senturk, S. *et al.* Rapid and tunable method to temporally control gene editing based on conditional Cas9 stabilization. *Nat. Commun.* **8**, 14370 (2017).

40.   Addgene: pLKO.1 – TRC Cloning Vector. Available at: https://www.addgene.org/tools/protocols/plko/. (Accessed: 17th June 2019)

41.   Addgene: pMD2.G. Available at: https://www.addgene.org/12259/. (Accessed: 17th June 2019)

42.   Addgene: psPAX2. Available at: https://www.addgene.org/12260/. (Accessed: 17th June 2019)

43.   Yuzugullu, H. *et al.* Canonical Wnt signaling is antagonized by noncanonical Wnt5a in hepatocellular carcinoma cells. *Mol. Cancer* **8**, 90 (2009).

44.   Giacinti, C. & Giordano, A. RB and cell cycle progression. *Oncogene* **25**, 5220–5227 (2006).

45.   Verhoeft, K. R., Ngan, H. L. & Lui, V. W. Y. The cylindromatosis (CYLD) gene and head and neck tumorigenesis. *Cancers Head Neck* **1**, 10 (2016).

46.   Das, M., Garlick, D. S., Greiner, D. L. & Davis, R. J. The role of JNK in the development of hepatocellular carcinoma. *Genes Dev.* **25**, 634–645 (2011).

47.   Malina, A. *et al.* PAM multiplicity marks genomic target sites as inhibitory to CRISPR-Cas9 editing. *Nat. Commun.* **6**, (2015).

7. <u>APPENDIX</u>

ASLI KURDEN PEKMEZCİ

Personal Information

Contact Information

Identity Number	69565113624
Date of Birth	17/08/1992
Contact Address	İzmir Biyotıp Ve Genom Merkezi Dokuz Eylül Üniversitesi Sağlık Kampüsü
Telephone	(545) 447 97 17
Email	aslikurden@gmail.com
Web Address	

Education Information

01 September 2016 – Now (2 Year 11 Month)
Yüksek Lisans, Tezli Program, DOKUZ EYLÜL ÜNİVERSİTESİ, TÜRKİYE
İZMİR ULUSLARARASI BİYOTIP VE GENOM ENSTİTÜSÜ, GENOM BİLİMLERİ VE MOLEKÜLER BİYOTEKNOLOJİ ANABİLİM DALI

01 September 2010 – 01 June 2015 (4 Year 10 Month)
Lisans, Anadal/Normal Öğretim, İZMİR YÜKSEK TEKNOLOJİ ENSTİTÜSÜ, TÜRKİYE
FEN FAKÜLTESİ, MOLEKÜLER BİYOLOJİ VE GENETİK BÖLÜMÜ

01 September 2006 – 01 June 2010 (3 Year 10 Month)
MİLLİ EĞİTİM BAKANLIĞI İL MİLLİ EĞİTİM MÜDÜRLÜKLERİ VE OKULLAR UŞAK İLİNDEKİ OKULLAR İL MERKEZİNDEKİ OKULLAR UŞAK FEN LİSESİ, TÜRKİYE

Foreign Language Information

İNGİLİZCE (Reading: İyi, Writing: İyi, Speaking: İyi)

R&D Competency

Conference Papers

A. KURDEN PEKMEZCİ & Ş. ŞENTÜRK, MALT1 PARAKASPAZIN HSK HÜCRE SAĞKALIMI ÜZERİNDEKİ ROLÜNÜN ARAŞTIRILMASI, Poster Sunumu, 3. Çukurova Hepatoselüler Karsinoma Kongresi, 21 February 2019, 23 February 2019.

A. KURDEN PEKMEZCİ & Ş. ŞENTÜRK, The Role of MALT1 Paracaspase in Hepatocellular Carcinoma, Poster Sunumu, 6th International Congress of the Molecular Biology Association of Turkey, 05 September 2018, 08 September 2018.

TÜBİTAK Scholarships and Fundings

Project Info	113S700, Bor Ve Türevlerinin Benign Prostat Hiperplazisi (Bph) Üzerine Anti-Proliferatif Ve Anti-Enflamatuvar Etki Mekanizmasının Araştırılması, 1001 – Araştırma, Burslu, Sonuçlandı, ARDEB, SBAG – Sağlık Bilimleri Araştırma Destek Grubu, Project Participation/Leave Dates: 2/23/16 – 5/30/16, Project Start/End Dates: 4/1/14 – 4/1/17. 117Z227, Malign Plevral Mezotelyoma Gelişiminde Rol Oynayan Esansiyel Genlerin ve Hücresel Yolakların CRISPR/Cas9 Güdümlü Tüm Genom Negatif Seçilim Tarama Yöntemiyle Sistematik Olarak Sorgulanması, Aydınlatılması ve Moleküler Karakterizasyonu, 3501 – Kariyer, Burslu, Yürürlükte, ARDEB, KBAG – Kimya Biyoloji Araştırma Destek Grubu, Project Participation/Leave Dates: 1/5/18 – 10/1/20, Project Start/End Dates: 10/1/17 – 10/1/20.
BIDEB Supports	ASLI KURDEN PEKMEZCİ, Etkinlik Destekleri ve Eğitim Bursları Müdürlüğü, 2210-A Genel Yurt İçi Yüksek Lisans Burs Programı, Başvurusu Reddedildi, 2017 – 2.

Number of Panelist/Observer/Reporter Jobs

Panelist/Outer Consultant Count	ARDEB/BİDEB 0	TEYDEB 0	Total 0
Number of Observer/Consultant Jobs	ARDEB/BİDEB 0	TEYDEB 0	Total 0
Number of Reporter Jobs	ARDEB/BİDEB 0	TEYDEB 0	Total 0